



1 **Identifying biological sources and indicators of surfactants in the sea**
2 **surface microlayer and subsurface waters using fluorescence and**
3 **microbial community profiling**

4 Felix E. Agblemanyo¹, Daniel Ammer², Amber E. Birt², Malique R. Bowen¹, Jennifer F. Biddle¹,
5 Amanda A. Frossard², Andrew S. Wozniak¹

6

7 ¹University of Delaware, School of Marine Science and Policy

8 ²University of Georgia, Department of Chemistry

9

10 Keywords: FDOM, surfactants, bacteria, protist, sea surface microlayer, microbial ecology,
11 northwestern Atlantic Ocean

12

13

14 *Correspondence to: Andrew Wozniak (awozniak@udel.edu); Felix Agblemanyo*
15 *(fedufia@udel.edu)*

16

17

18

19

20



21 **Abstract**

22 Marine surfactants accumulate in the sea surface microlayer (SML) where they influence gas
23 transfer velocities and air-sea exchange of climate relevant gases. Despite their importance, the
24 biological sources and reliable proxies of marine surfactants remain poorly constrained. This study
25 paired measurements of surfactant concentrations and fluorescent dissolved organic matter
26 (FDOM) composition with bacterial and protist community profiles in the SML and subsurface
27 waters (SSW) across three hydrographic regions and two seasons in the northwestern Atlantic
28 Ocean. Surfactant concentrations were significantly enriched in the SML relative to the SSW, and
29 temporal differences are a major driver of variability in surfactant concentrations, as demonstrated
30 by the highest values recorded during a fall picoeukaryotic bloom. Surfactant concentrations
31 showed a positive correlation with tryptophan-like FDOM, supporting a biogenic source of marine
32 surfactants. Microbial community composition differed between the SML and SSW, with the SML
33 enriched in small, resource-efficient taxa adapted to high-light and low-nutrient conditions.
34 Significant correlations were observed between surfactant concentrations and diverse microbial
35 taxa, including picoeukaryotic phytoplankton such as *Ostreococcus*, *Bathycoccus*, and
36 *Micromonas*; heterotrophic bacteria such as the NS5 marine group, *Pseudoalteromonas*, SAR86,
37 and *Candidatus Actinomarina*; as well as phagotrophic protists such as MAST-7B and Cercozoa,
38 and parasitic dinoflagellates from the Dino-Group-I and Dino-Group-II clades. The diversity of
39 surfactant associated microbial candidates suggests that surfactant production reflects a broader
40 range of microbial processes than phytoplankton activity alone, with tryptophan-like FDOM
41 capturing this integrated biological process more effectively than chlorophyll-a concentrations.
42 These findings establish tryptophan-like FDOM as a promising proxy for predicting marine



43 surfactant concentrations and highlight the need for an in-depth understanding of the diverse

44 microbial sources of surfactants.



45 **1 Introduction**

46 Surfactants are amphiphilic organic compounds composed of a hydrophilic moiety and a
47 hydrophobic moiety. They are typically characterized by lower oxygen-to-carbon and higher
48 hydrogen-to-carbon ratios relative to bulk dissolved organic matter (DOM) (Burdette et al., 2022;
49 Coffey et al., 2025) and include a wide range of compounds such as phospholipids, amino acids,
50 fatty acids, alkyl sulfates and linear alkylbenzene sulfonates (Frew et al., 2006; Cochran et al.,
51 2016; Barthelmeß and Engel, 2022). Due to their amphiphilic nature, they tend to adsorb at air-
52 water interfaces like bubbles and the sea surface microlayer (SML). The SML is the topmost 10s
53 to 100s μm thick layer of the ocean with distinct physicochemical and biological characteristics
54 compared to underlying subsurface waters (SSW) (Zhang et al., 2003; Cunliffe et al., 2013; Ebling
55 and Landing, 2015; Wurl et al., 2018; Burdette et al., 2022; Coffey et al., 2025). Surfactants in the
56 SML influence gas transfer velocities, aerosol particle emissions and subsequent cloud droplet
57 formation, and trace gas uptake at the ocean surface (Hoffman and Duce, 1976; Wilson et al.,
58 2015). These surfactant effects may be a source of inaccuracies in existing global climate models,
59 creating a need for effective proxies for estimating the spatiotemporal variability of surfactants
60 and their impact on air-sea processes (Pereira et al., 2018).

61 In the ocean, surfactants are primarily derived from biological sources, including bacterial
62 and phytoplankton exudates (Zutic et al., 1981; Hardy, 1982; Liu et al., 2023). Several studies have
63 linked increases in surfactant concentrations to high primary productivity, particularly during
64 phytoplankton bloom seasons (Gašparović and Čosović, 2003; Gašparović et al., 2007; Frka et al.,
65 2009; Wurl et al., 2011). Surface slicks have also been associated with the presence of specific
66 groups of surfactant-producing bacteria (Kurata et al., 2016). These bacteria are thought to be
67 primarily hydrocarbon degrading groups such as *Bacillus*, *Paracoccus*, and *Pseudoalteromonas*,



68 which synthesize biosurfactants that facilitate the solubilization and uptake of hydrophobic
69 substrates (Maneerat et al., 2006; Antoniou et al., 2015; Morales-Guzmán et al., 2021). Additional
70 biological contributions may arise from processes such as protist grazing, parasitism, and viral
71 lysis, although these pathways remain relatively unexplored. Surfactants can also originate from
72 terrestrial and anthropogenic sources, including plant-derived compounds (e.g., saponins) (Rai et
73 al., 2021), microbial biosurfactants transported from sediments (Morales-Guzmán et al., 2021),
74 and anthropogenic inputs such as linear alkylbenzene sulfonates and per- and polyfluoroalkyl
75 substances (PFAS) (Jardak et al., 2016). Despite these diverse sources, their relative contributions
76 to surfactant concentrations and composition, and their impact on air-sea processes, are not well
77 understood. In addition, there remain gaps in the specific microbial communities contributing to
78 surfactant concentrations. Identifying these diverse microbial sources is important because their
79 spatiotemporal abundance can be linked to surfactant concentrations and composition, which are
80 known to influence the magnitude of surfactant effects on air-sea processes (Frossard et al., 2019;
81 Burdette et al., 2022; El Haber et al., 2024).

82 Fluorescent dissolved organic matter (FDOM) constitutes a subset of DOM that fluoresces
83 under ultraviolet (UV) light (Stedmon and Bro, 2008). The study of FDOM using
84 spectrofluorometry provides a relatively fast and cost-effective approach for tracking organic
85 matter sources and transformations in aquatic ecosystems (Huguet et al., 2009). FDOM spans a
86 range of biological and terrestrial origins and is broadly categorized into humic-like and protein-
87 like components. Humic-like components are typically associated with terrestrially derived and
88 degraded organic matter, whereas protein-like components are linked to both photosynthetic and
89 heterotrophic microbial activity and are considered indicators of recently produced autochthonous
90 organic matter (Coble, 1996; Stedmon and Markager, 2005; Yamashita et al., 2015; Devresse et



91 al., 2023). Establishing relationships between FDOM composition and surfactant concentrations
92 may therefore help infer the relative contributions of biological versus terrestrial sources of
93 surfactants. In addition, tryptophan-like FDOM has been positively correlated with surfactant-like
94 DOM, including unsaturated aliphatics, peptide-like compounds, and sulfur-rich compounds
95 (Coffey et al., 2025), suggesting that it may serve as a proxy for surfactant abundance in marine
96 systems.

97 Amplicon sequencing of marker genes, including the 16S rRNA gene for bacteria and the
98 18S rRNA gene for protists, enables high-resolution characterization of microbial community
99 composition across diverse environments. Such approaches have identified dominant SML taxa,
100 including bacterial groups such as Proteobacteria, Cyanobacteria, Actinobacteria, and
101 Bacteroidetes (Cunliffe et al., 2011; Rahlff et al., 2021; Tastassa et al., 2025), as well as protists
102 including Alveolata, Chrysophyceae, and Stramenopiles (Taylor and Cunliffe, 2014; Zäncker et
103 al., 2021). Seasonal and spatial variations in these communities have also been reported (Čanković
104 et al., 2022; Liu et al., 2023); however, studies that simultaneously measure microbial community
105 structure alongside surfactant concentrations are limited. Linking microbial community structure
106 with surfactant concentrations across contrasting hydrographic regions and seasons will help
107 identify key biological indicators and potential surfactant producing taxa, providing new insight
108 into the microbial processes that regulate surfactant variability in the ocean.

109 In this study, we characterize the bacterial and protist communities through 16S rRNA and
110 18S rRNA gene amplicon sequencing, respectively, in the SML and SSW at three sites in the
111 Northwestern Atlantic during the summer and fall of 2022, and we assess their temporal and spatial
112 variations. Concurrent measurements of surfactant concentrations and FDOM composition were
113 paired with the microbial community data to identify biogenic and terrestrial contributions to



114 surfactant pools and to detect potential microbial biomarkers and candidate surfactant producing
115 taxa.

116

117 **2 Methods**

118 **2.1 Sampling Locations**

119 Two research cruises were conducted in summer (August 24 – September 2) and fall
120 (November 10 – 11) 2022 to collect SML and SSW samples from the northwestern Atlantic Ocean
121 aboard the *R/V Hugh R. Sharp*. Details about the project and sampling sites are outlined by
122 Agblemanyo et al. (2026) and briefly described here. During the summer cruise, three sites were
123 sampled, including a Delaware Coast station (38.72, -74.75), a Virginia Coast station (37.81, -
124 75.42), and a Continental Slope station (37.83, -73.72). In the fall, only the Delaware Coast station
125 was sampled because the cruise was cut short, as it coincided with Hurricane Ian. These sampling
126 sites were chosen to span a range of terrestrial/marine influences and biological productivities. The
127 Virginia Coast station is the closest to land and is impacted by the Chincoteague Bay, while the
128 Continental Slope station is the farthest offshore. The Delaware Coast station is farther from land
129 than the Virginia Coast station and is also directly impacted by the Delaware Bay. The two coastal
130 stations represent sites with higher terrestrial influence, whereas the Continental Slope station
131 represents marine conditions.

132 **2.2 SML and SSW Sample Collection**

133 SML samples were collected using the rosette-based glass plate (RGP) sampler. The RGP
134 sampler was made up of three large glass plates (66 x 76 cm) attached to the metal frame of a 24-
135 bottle rosette sampler and was controlled using the A-frame and mechanical winch system of the



136 *R/V Hugh R. Sharp*. A detailed description of the RGP sampler, which enables safe, ship-based
137 deployment of the sampler for the collection of high volume ($\sim 1 \text{ L h}^{-1}$) samples, is provided by
138 Agblemanyo et al. (2026). SSW samples were collected from $\sim 0.5 \text{ m}$ depth using a modified pump
139 profiler system (Hudson et al., 2019) from the starboard side of the ship directly after sampling the
140 SML. These paired SML and SSW samples were collected three times throughout the day at each
141 sampling station, including afternoon ($\sim 13:00$), evening ($\sim 18:30$) and night ($\sim 02:30$), with a small
142 number of stations also including a morning ($\sim 10:00$) sample. Only three samples were obtained
143 from the Virginia Coast station due to storm conditions during sampling. Sample metadata and
144 environmental parameters are provided in Table S1.

145 **2.3 Dissolved Organic Matter Measurements**

146 DOM characteristics, including FDOM composition, surfactant concentrations, and
147 dissolved organic carbon (DOC) concentrations were measured for the collected SML and SSW
148 samples. For all DOM analyses, samples were filtered immediately after collection using pre-
149 combusted ($450 \text{ }^\circ\text{C}$, 4 h) $0.7 \text{ }\mu\text{m}$ pore size glass fiber filters and stored for subsequent analysis.

150 Anionic surfactant concentrations were determined using $\sim 100 \text{ mL}$ of filtered samples.
151 Samples were solid phase extracted on the ship using ENVI-18 cartridges (C18 sorbent material,
152 0.5 g bed weight, Millipore Sigma). The cartridges containing the retained extracts were stored at
153 $-20 \text{ }^\circ\text{C}$ until elution in the lab. Surfactant concentrations were subsequently quantified using the
154 colorimetric method according to established protocols (Gérard et al., 2016; Frossard et al., 2019;
155 Burdette and Frossard, 2021; Bramblett and Frossard, 2024).

156 Aliquots of the filtered samples ($\sim 10 \text{ mL}$) were stored at $4 \text{ }^\circ\text{C}$ for FDOM analysis and were
157 analyzed within two weeks of sample collection. Fluorescence excitation emission matrices



158 (EEMs) of the samples were obtained using a HORIBA Aqualog® spectrofluorometer across
159 excitation and emission wavelength ranges of 230 – 700 nm and 245 – 822 nm, respectively.
160 Readings were acquired at intervals of 2 nm for excitation and 4.65 nm for emission. EEMs data
161 were corrected for inner filter effects and Raman calibrated (McKnight et al., 2001; Lawaetz and
162 Stedmon, 2009). Parallel factor analysis (PARAFAC) was then used to deconvolute fluorescent
163 components across samples using R packages *starDom* and *eemR* (Ohno, 2002; Pucher et al., 2019;
164 Ouyang et al., 2024). The resulting components were validated by comparison with reference
165 spectra in the OpenFluor database (Murphy et al., 2014) (Table S2).

166 For DOC analysis, ~20 mL of the filtered samples were acidified to pH 2 using 2 M HCl
167 and then purged to remove inorganic carbon. DOC concentrations were then measured by high
168 temperature (680 °C) catalytic oxidation (Emery et al., 1971; Sharp et al., 1993) using a Shimadzu
169 TOC-Vcph analyzer. Calibration curves generated from potassium hydrogen phthalate standards
170 were used to quantify DOC mass concentrations (mg of DOC per L). A detailed description of the
171 DOC concentrations of these samples have already been published (Agblemany et al., 2026). In
172 this study, the DOC concentrations were used to normalize the FDOM and surfactant
173 concentrations, and throughout the text, surfactant concentrations are reported as μmol surfactant
174 per mg DOC, while FDOM concentrations are reported as Raman Units (RU) per mg DOC.

175 **2.4 DNA Extraction, Sequencing and Analysis**

176 The collected SML and SSW water samples (~200 mL) were also filtered right after
177 sampling using 0.22 μm nitrocellulose membrane filters. The filters were wrapped in
178 precombusted aluminum foil packets and stored at -80 °C until DNA extraction. Genomic DNA
179 was extracted from the filters using the DNeasy® PowerSoil® (QIAGEN, Georgetown, MD,
180 USA) Pro Kit following manufacturer's instructions. The V4 regions of the 16S and 18S rRNA



181 genes were amplified using the 515F (5'-GTG-CCA-GCM-GCC-GCG-GTA-A-3') and 806R (5'-
182 GGA-CTA-CHV-GGG-TWT-CTA-AT-3') primers (Caporaso et al., 2012) for bacteria, and the
183 TAReuk_F (5'-CCA-GCA-SCY-GCG-GTA-ATT-CC-3') and TAReuk_R (5'-ACT-TTC-GTT-
184 CTT-GAT-YRA-3') primers (STOECK et al., 2010) for protists, respectively. The amplified
185 products were then sequenced on the MiSeq platform (Illumina, Inc., San Diego, CA, USA) at the
186 Microbial Analysis, Resources, and Services (MARS) facility of the University of Connecticut
187 following their standard protocols (Chen et al., 2023).

188 Bioinformatics analyses were conducted using the Mothur v.1.48.0 pipeline (Kozich et al.,
189 2013). Paired end reads were assembled into contigs, screened for chimeras, and unique sequences
190 were assigned as amplicon sequence variants (ASVs). Taxonomic classification of the bacteria 16S
191 rRNA gene sequences was performed using the SILVA version 138.2 database (Quast et al., 2012)
192 for bacteria, while protist 18S rRNA gene sequences were classified using the PR² version 5.1.1
193 database (Guillou et al., 2012; González-Miguéns et al., 2025). The number of sequences were
194 normalized by subsampling to 10,054 sequences per sample for bacteria and 1,072 sequences per
195 sample for protists, after removing an SML and an SSW protist sample which had less than 1000
196 reads. Chloroplast, mitochondria, archaea and eukaryotic sequences present in the 16S rRNA gene
197 dataset were removed, whereas metazoan and higher plant sequences were removed from the 18S
198 rRNA gene dataset. ASVs not present in more than 5% of samples were also removed.

199 **2.5 Additional Oceanographic Measurements**

200 Sea surface salinity and temperature were measured and recorded continuously with
201 shipboard instrumentation (SBE 45, Sea-Bird, at 3.7 m depth) and were averaged for the times at
202 which samples were collected. Chlorophyll-*a* (chl-*a*) concentrations were measured continuously
203 with the shipboard fluorometer (AU10, Turner). The shipboard fluorometer measurements were



204 calibrated using the chl-*a* concentrations of discrete samples that were measured in the lab using
205 the spectrophotometric method described by Aminot and Rey (2000).

206 **2.6 Statistical Analyses**

207 Statistical similarities and differences in DOM (surfactant concentrations and FDOM
208 composition) between the SML and SSW were assessed using the Wilcoxon rank-sum test (two
209 independent data sets) and across stations using the Kruskal-Wallis test (four independent data
210 sets). Correlations between surfactant concentrations and FDOM components were determined
211 using Pearson correlation analysis.

212 Microbial ASV sequence counts were converted to relative abundances for visualization.
213 For statistical analyses, ASV counts were centered log-ratio (clr) transformed to account for
214 compositionality using the *compositions* package (van den Boogaart and Tolosana-Delgado,
215 2008). Differences in microbial community composition were estimated using Bray-Curtis
216 dissimilarities and visualized via principal coordinates analysis (PCoA) using the *vegan* package
217 (Oksanen et al., 2022). Differences in microbial community structure between sample types and
218 among stations were also tested using permutational analysis of variance (PERMANOVA).
219 Indicator species analysis was then conducted using the *multipatt* function in the *indicspecies*
220 package (De Cáceres and Legendre, 2009) to identify specific ASVs significantly associated ($p <$
221 0.05) with either the SML or SSW or with the different stations.

222 General relationships between DOM variables and microbial community structure were
223 examined using distance-based redundancy analysis (dbRDA). Correlation network analysis was
224 then used to identify significant associations between ASVs and DOM variables (surfactant
225 concentrations and FDOM components) based on Pearson correlations ($p < 0.05$). Networks were

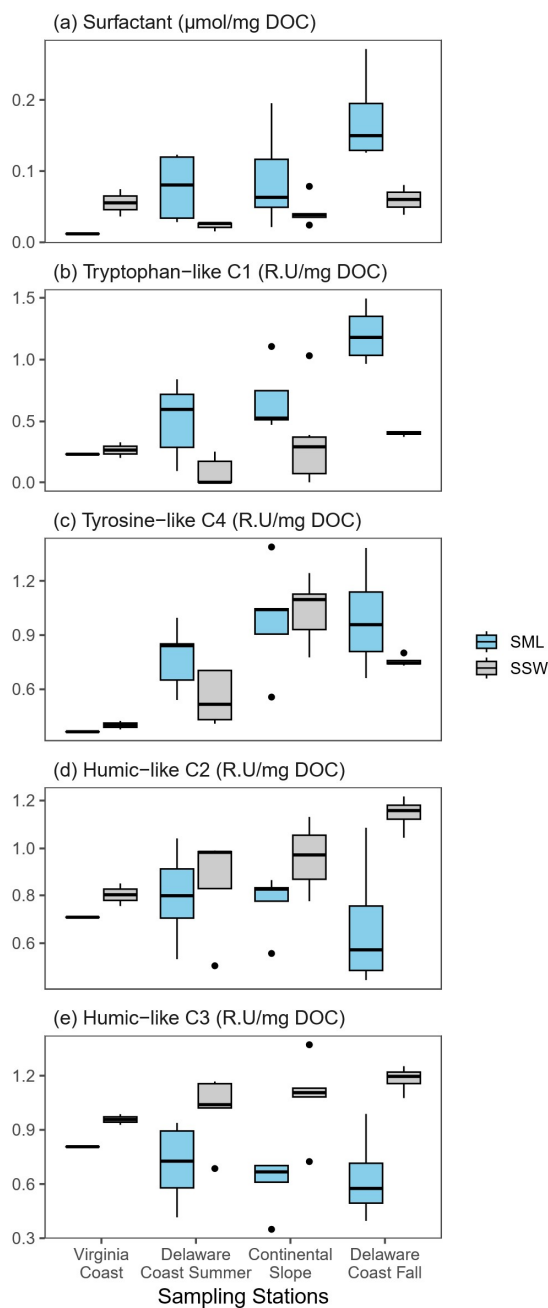


226 constructed and visualized using the *igraph* (Csárdi and Nepusz, 2006) and *ggraph* (Pedersen,
227 2022) packages, where nodes represent ASVs or DOM variables, and edges represent significant
228 correlations. Network structure was characterized by modularity (Q) and was calculated using the
229 *bipartite* package (Dormann et al., 2009).

230 **3 Results**

231 **3.1 Physicochemical Properties of Sampling Stations**

232 The average salinities during summer sampling were 32.5 ± 0.03 , 32.4 ± 0.20 and $33.2 \pm$
233 0.20 ppt and average chl-*a* concentrations were 2.20 ± 0.67 , 0.36 ± 0.15 and $0.25 \pm 0.10 \mu\text{g L}^{-1}$
234 for the Virginia Coast, Delaware Coast and Continental Slope stations, respectively. The
235 Continental Slope station, which was farthest from land, had the highest salinity compared to the
236 two coastal stations. The Virginia Coast station had the highest chl-*a* concentration in the summer,
237 followed by the Delaware Coast with the Continental Slope station having the lowest. During the
238 fall sampling at the Delaware Coast station, average salinity and chl-*a* concentration was $33.0 \pm$
239 0.10 ppt and $2.74 \pm 0.98 \mu\text{g L}^{-1}$, respectively. The Delaware Coast chl-*a* concentration in the fall
240 was the highest compared to all other sites, indicating a potential bloom during the fall sampling.



241

242 **Figure 1:** Different fractions of DOM normalized by DOC in SML and SSW measured at the four
243 sampling stations, including (a) surfactant concentrations (μmol surfactant per mg DOC) and
244 PARAFAC FDOM components (with units of RU per mg DOC) including tryptophan-like C1(b),
245 tyrosine-like C4 (c), marine humic-like C2 (d), and terrestrial humic-like C3 (e).



246 3.2 Surfactant Concentrations in SML and SSW

247 Surfactant concentrations (Figure 1a) were significantly higher (Wilcoxon, $p = 0.028$) in
248 the SML (mean of $0.10 \pm 0.07 \mu\text{mol surfactant mg}^{-1} \text{DOC}$, $n = 16$) compared to the SSW (mean of
249 $0.04 \pm 0.02 \mu\text{mol surfactant mg}^{-1} \text{DOC}$, $n = 13$) across all of the sampling locations and dates,
250 which supports their preferential accumulation in the SML. Surfactant concentrations were not
251 significantly different in either the SML or SSW across the summer sampling stations (Kruskal-
252 Wallis, $p > 0.05$). However, the SML surfactant concentrations were generally higher at the
253 Continental Slope ($0.09 \pm 0.07 \mu\text{mol surfactant mg}^{-1} \text{DOC}$), followed by Delaware Coast ($0.08 \pm$
254 $0.05 \mu\text{mol surfactant mg}^{-1} \text{DOC}$), and then Virginia Coast ($0.01 \mu\text{mol surfactant mg}^{-1} \text{DOC}$). In
255 the SSW, surfactant concentrations generally declined from Virginia Coast ($0.06 \pm 0.03 \mu\text{mol}$
256 $\text{surfactant mg}^{-1} \text{DOC}$) to Continental Slope ($0.04 \pm 0.02 \mu\text{mol surfactant mg}^{-1} \text{DOC}$) and Delaware
257 Coast ($0.02 \pm 0.01 \mu\text{mol surfactant mg}^{-1} \text{DOC}$). Additionally, there were significant seasonal
258 differences in the surfactant concentrations of the Delaware Coast fall and summer samples
259 (Kruskal-Wallis, $p < 0.05$). SML surfactant concentrations more than doubled from summer (0.08
260 $\pm 0.05 \mu\text{mol surfactant mg}^{-1} \text{DOC}$) to fall ($0.17 \pm 0.07 \mu\text{mol surfactant mg}^{-1} \text{DOC}$), and SSW
261 concentrations similarly increased from summer ($0.02 \pm 0.01 \mu\text{mol surfactant mg}^{-1} \text{DOC}$) to fall
262 ($0.06 \pm 0.02 \mu\text{mol surfactant mg}^{-1} \text{DOC}$). This seasonal increase indicates higher release of
263 surfactants during the fall bloom.

264 3.3 FDOM composition in SML and SSW

265 PARAFAC analysis of the fluorescence EEMs data identified four major FDOM
266 components (C1 to C4) across all samples, which included two protein-like and two humic-
267 components (Table S2). The protein-like components were identified as tryptophan-like (C1,
268 $\text{ex/em} = 276/339 \text{ nm}$) and tyrosine-like (C4, $\text{ex/em} = 276/309$) FDOM, and the two humic-like



269 peaks were identified as marine humic-like (C2, ex/em = 250/395) and terrestrial humic-like (C3,
270 259/464) FDOM (Coble, 1996, 2007). The protein-like components indicate freshly produced or
271 autochthonous biological DOM (Coble, 1996, 2007). The marine humic-like component C2 are
272 associated with microbial reprocessed DOM, whereas the terrestrial humic-like component C3 are
273 associated with high aromatic and humic substances from soils and vascular plants (Coble, 1996,
274 2007).

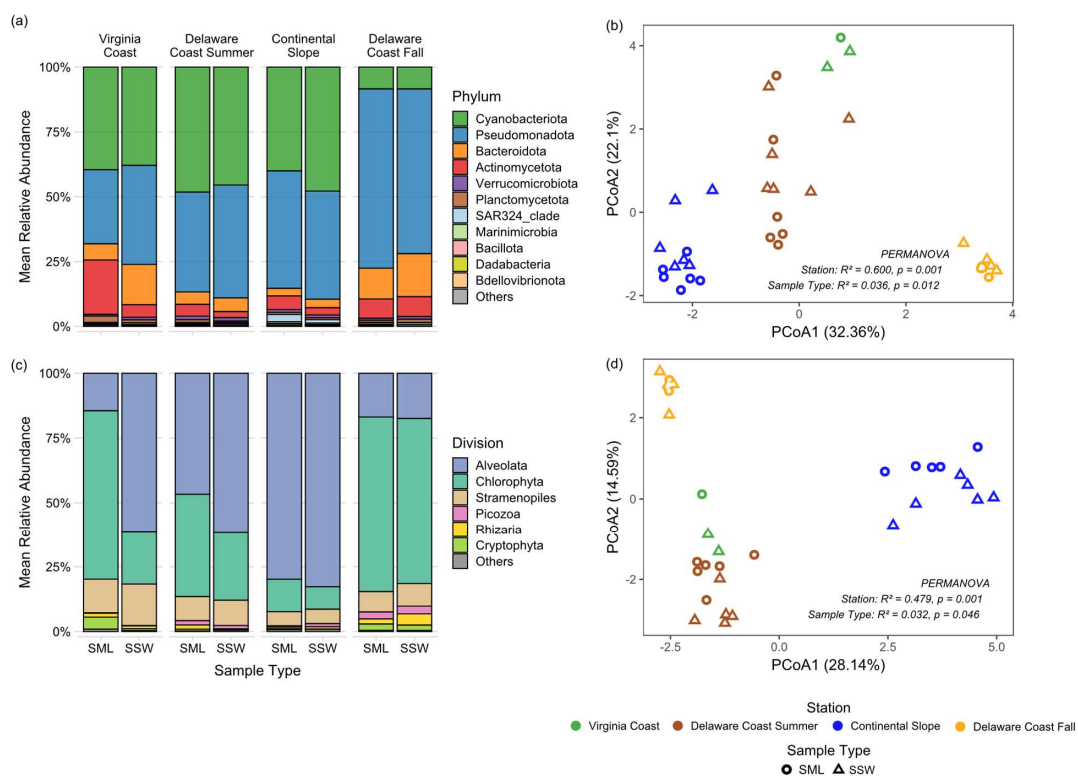
275 The tryptophan-like C1 (Figure 1b) was significantly more abundant in the SML compared
276 to the SSW (Kruskal-Wallis, $p < 0.05$), whereas the tyrosine-like C4 (Figure 1c) was not
277 significantly different between the two layers. In contrast, the humic-like C2 (Figure 1d) and C3
278 (Figure 1e) components were significantly more abundant in the SSW (Kruskal-Wallis, $p < 0.05$),
279 signifying higher relative quantities of aromatic and humified DOM in SSW compared to the SML.
280 Tyrosine-like C4 was the only FDOM component that differed significantly across summer
281 stations, showing lower abundance at the Virginia Coast than at the Continental Slope (Kruskal-
282 Wallis, $p = 0.0006$). Similarly to surfactant concentrations, the tryptophan-like C1 displayed
283 significantly higher abundance in fall compared to summer at the Delaware Coast station (Kruskal-
284 Wallis, $p = 0.023$), whereas the remaining FDOM components were statistically similar across the
285 two seasons.

286 **3.4 Relationships between FDOM Components and Surfactant Concentrations**

287 Surfactant concentrations were significantly, positively correlated with the tryptophan-like
288 C1 ($r = 0.68$, $p < 0.05$) and significantly, negatively correlated with the terrestrial humic-like C3
289 component ($r = -0.43$, $p < 0.05$) (Figure S1). This suggests that the processes and conditions that
290 produce tryptophan-like FDOM also yield enhanced surfactant concentrations. Given a presumed



291 biological source for C1 (Coble, 1996, 2007), this observation supports the biological and marine
 292 source of surfactant-like compounds in the SML.



293
 294 **Figure 2:** Microbial community structure of bacteria and protists in the SML and SSW across
 295 sampling stations. (a) Mean relative abundance of bacterial phyla and (c) protist divisions across
 296 all samples collected at each site. PCoA based on Bray-Curtis dissimilarity of (b) bacterial and (d)
 297 protist communities. PERMANOVA results are shown for the effects of station and sample type
 298 on the microbial communities.

299 3.5 General Microbial Community Structure

300 Amplicon sequencing of the 16S and 18S rRNA genes identified 1127 bacterial ASVs and
 301 481 protist ASVs across all samples, representing unique microbial lineages and suggesting higher
 302 bacterial diversity relative to protist communities. The most abundant microbial groups across all
 303 stations in both the SML and SSW samples included the bacterial phyla Pseudomonadota,
 304 Cyanobacteriota, Bacteroidota, and Actinomycetota, as well as the protist divisions Alveolata,



305 Chlorophyta, and Stramenopiles (Figures 2a & 2c). On average, Pseudomonadota (47%),
306 Cyanobacteriota (36.3%), Bacteroidota (7%), and Actinomycetota (5%) made up more than 95%
307 of the bacteria phyla in this study (Figure 2a), whereas Alveolata (53%), Chlorophyta (34%) and
308 Stramenopiles (8%) together made up 92% of the protist divisions (Figure 2c).

309 The microbial communities varied significantly between the SML and SSW and between
310 the different stations/seasons (PERMANOVA, $p < 0.05$), as observed by the distinct clustering in
311 the principal coordinate analysis (PCoA) (Figures 2b & 2d). For bacterial communities, the first
312 PCoA axis (explaining 32.4% of variance) captured seasonal variation, as shown by the clustering
313 of the Delaware Coast fall samples on the positive end of PCoA1 and summer samples clustered
314 toward the negative end of PCoA1. The second axis (22.1%) reflected spatial differences that are
315 related to proximity to shore and salinity, as observed by the Continental Slope samples clustering
316 at the negative end of PCoA2 while the Delaware Coast and Virginia Coast samples clustered
317 toward the positive end of PCoA2 (Figure 2b). In protist communities, the first axis explained
318 27.1% of the variation and was primarily associated with spatial differences, as can be seen by the
319 clear separation of Continental Slope samples on the positive end of PCoA1 from the Virginia
320 Coast and Delaware Coast samples clustering on the negative end. The second axis (14.6%)
321 captured seasonal variation as noted by the separation of Delaware Coast fall samples on the
322 positive PCoA2 from the summer samples which clustered toward the negative PCoA2 (Figure
323 2d).

324 These compositional variations are observed at the phylum/division level. For example,
325 Chlorophyta was consistently more abundant in the SML across all samples (Figure 2c), and
326 Actinomycetota was similarly enriched in the SML in the summer samples, though this pattern



327 was less pronounced in the fall (Figure 2a). In contrast, the bacterial phylum Bacteroidota and the
328 protist division Alveolata were more abundant in the SSW across all samples.

329 Across the summer stations, Bacteroidota was more abundant at the coastal stations
330 (Delaware Coast and Virginia Coast) compared to the Continental Slope, whereas SAR324
331 (Marine Group B) was more prevalent at the Continental Slope station (Figure 2a). Among protists,
332 Alveolata was more abundant offshore, while Chlorophyta and Stramenopiles increased at the
333 coastal stations (Figure 2c). Seasonal patterns at the Delaware Coast station showed increases in
334 Pseudomonadota, Actinomycetota, and Bacteroidota in the fall, while Cyanobacteriota decreased
335 (Figure 2a). The protist groups Chlorophyta and Cryptophyta also increased in fall, while Alveolata
336 decreased (Figure 2c). The compositional differences are explored in further detail at the ASV
337 level in subsequent sections.

338



339 **Table 1:** Phylum and genus of the top 10 most abundant bacterial lineages (ASVs) significantly
 340 associated with the SML or SSW, with mean abundance, association strength, and P value (full list
 341 of significant taxa is provided in Table S3).

Phylum	Genus	ASV	Mean Abundance (%) [*]	Association Strength (r.g) ⁺	P value
SML Associated Taxa					
Actinomycetota	<i>Candidatus Actinomarina</i>	ASV010	2.51	0.35	0.015
Pseudomonadota	SAR86 clade	ASV008	2.11	0.26	0.02
Pseudomonadota	SAR86 clade	ASV013	2.06	0.30	0.006
Pseudomonadota	SAR86 clade	ASV014	1.38	0.16	0.046
Pseudomonadota	<i>Candidatus Puniceispirillum</i>	ASV031	0.92	0.36	0.001
Pseudomonadota	SAR116 clade	ASV020	0.90	0.21	0.013
Pseudomonadota	AEGEAN-169 marine group	ASV030	0.83	0.28	0.032
Pseudomonadota	<i>Paracoccaceae</i>	ASV026	0.74	0.21	0.047
Pseudomonadota	AEGEAN-169 marine group	ASV040	0.74	0.34	0.013
Pseudomonadota	SAR86 clade	ASV044	0.58	0.31	0.006
SSW Associated Taxa					
Pseudomonadota	<i>Caulobacter</i>	ASV009	4.80	0.39	0.001
Bacteroidota	NS5 marine group	ASV017	1.22	0.11	0.042
Pseudomonadota	<i>Alteromonas</i>	ASV038	0.98	0.29	0.049
Pseudomonadota	<i>Cupriavidus</i>	ASV059	0.82	0.44	0.001
Pseudomonadota	<i>Comamonadaceae</i>	ASV079	0.47	0.30	0.01
Bacteroidota	<i>Mesoflavibacter</i>	ASV130	0.33	0.29	0.002
Bacteroidota	<i>Cryomorphaceae</i>	ASV067	0.28	0.19	0.027
Pseudomonadota	<i>Thalassospira</i>	ASV207	0.21	0.39	0.002
Pseudomonadota	<i>Thalassolituus</i>	ASV290	0.21	0.31	0.014
Bacteroidota	<i>Fluviicola</i>	ASV072	0.18	0.23	0.006

342 ^{*}Mean relative abundance (%) of each ASV calculated within its associated sample type (SML or
 343 SSW).

344 ⁺Group-equalized point-biserial correlation coefficient (r.g) showing association strength between
 345 each ASV and sample type.

346 3.6 SML and SSW Associated Microbial Taxa

347 Indicator species analysis identified specific bacterial and protist lineages that were
 348 significantly associated either with the SML or SSW. A total of 30 bacterial ASVs (2.7% of
 349 bacterial ASVs) were associated with the SML, whereas 107 ASVs (9.5% of bacterial ASVs) were
 350 associated with SSW (Table S3). At the phylum level, a majority of both the SML and SSW
 351 associated bacteria ASVs belonged to Pseudomonadota, though the SML showed a higher



352 proportion of Pseudomonadota relative to SSW. The SSW associated bacteria were more diverse
353 and were dominated by ASVs of the phyla Bacteroidota and Cyanobacteria. However, while both
354 layers share bacteria at the phylum level, a more resolved taxonomic level reveals ecologically
355 distinct assemblages between the SML and SSW. Some of the abundant SML associated bacteria
356 lineages (Table 1) included those of SAR86 (ASV008, ASV013, ASV014, ASV044), *Candidatus*
357 *Actinomarina* (ASV010), SAR116 clade (ASV020), *Candidatus Puniceispirillum* (ASV031),
358 *Paracoccaceae* (ASV026), and AEGEAN-169 marine group (ASV030, ASV040), the majority of
359 which are photoheterotrophs found to be abundant in oligotrophic waters. Notable SSW associated
360 bacteria lineages (Table 1) included *Caulobacter* (ASV009), *Cupriavidus* (ASV059), *Alteromonas*
361 (ASV038), *Comamonadaceae* (ASV079) and *Mesoflavibacter* (ASV130), which are typically
362 associated with terrestrial and organic matter-rich environments.

363



364 **Table 2:** Division and genus of the top 10 most abundant protist lineages (ASVs) significantly
 365 associated with the SML or SSW, with mean abundance, association strength, and P value (full list
 366 of significant taxa is provided in Table S4).

Division	Genus	ASV	Mean Abundance (%) [*]	Association Strength (r.g) ⁺	P value
SML Associated Taxa					
Chlorophyta	<i>Ostreococcus</i>	ASV001	20.53	0.26	0.011
Chlorophyta	<i>Ostreococcus</i>	ASV034	2.82	0.30	0.023
Alveolata	Dino-Group-II-Clade-1_X	ASV183	0.91	0.35	0.017
Rhizaria	<i>Cryomonadida XX</i>	ASV488	0.55	0.27	0.028
Stramenopiles	<i>Phytophthora</i>	ASV1099	0.22	0.30	0.009
Alveolata	Dino-Group-II	ASV1402	0.18	0.30	0.039
Alveolata	Dino-Group-V XX	ASV184	0.16	0.36	0.005
Alveolata	Dino-Group-II-Clade-22 X	ASV850	0.14	0.31	0.04
Alveolata	<i>Prorocentrum</i>	ASV231	0.09	0.34	0.005
Alveolata	Dino-Group-II-Clade-12 X	ASV1232	0.08	0.36	0.015
SSW Associated Taxa					
Alveolata	<i>Gyrodinium</i>	ASV003	8.72	0.26	0.037
Alveolata	<i>Gyrodinium</i>	ASV021	2.62	0.42	0.003
Alveolata	<i>Strombidiidae X</i>	ASV162	1.16	0.41	0.001
Alveolata	<i>Laboea</i>	ASV043	0.65	0.38	0.001
Alveolata	<i>Gonyaulax</i>	ASV197	0.51	0.32	0.029
Alveolata	<i>Gyrodinium</i>	ASV046	0.50	0.38	0.016
Alveolata	<i>Strombidiidae X</i>	ASV073	0.31	0.36	0.039
Alveolata	<i>Strombidiidae X</i>	ASV247	0.25	0.45	0.002
Alveolata	<i>Spirotrichea</i>	ASV265	0.25	0.41	0.01
Alveolata	<i>Oligotrichida XX</i>	ASV373	0.21	0.43	0.003

367 ^{*}Mean relative abundance (%) of each ASV calculated within its associated sample type (SML or
 368 SSW).

369 ⁺Group-equalized point-biserial correlation coefficient (r.g) showing association strength between
 370 each ASV and sample type.

371 For protists, 23 (4.8% of protist ASVs) and 21 (4.4% of protist ASVs) protist lineages
 372 associated with the SML and SSW, respectively (Table S4). At the division level, Alveolata
 373 dominated the indicator ASV pool in both SML and SSW, with all SSW associated protist lineages
 374 belonging to Alveolata. Unlike bacteria, the SML associated protist lineages were more diverse
 375 than those of the SSW, with the SML protists additionally dominated by Chlorophyta,
 376 Stramenopiles and Rhizaria. At a more resolved taxonomic level, some of the abundant SML



377 enriched protist lineages (Table 2) were the green algae *Ostreococcus* (ASV001, ASV034), the
 378 dinoflagellates Dino-Group-II clades (ASV183, ASV1402, ASV200, ASV1232, ASV850) and
 379 Dino-Group-V (ASV184), and the heterotrophic flagellate *Cryomonadida* (ASV488). While those
 380 for the SSW were the mixotrophic dinoflagellates *Gyrodinium* (ASV003, ASV021, ASV046) and
 381 *Gonyaulax* (ASV197), the ciliates *Strombidiidae* (ASV162, ASV073, ASV247), *Spirotrichea*
 382 (ASV265), and *Laboea* (ASV043).

383 **Table 3:** Phylum and genus of the top 10 most abundant bacterial lineages (ASVs) significantly
 384 associated with each sampling station, with mean abundance, association strength, and P value
 385 (additional significant lineages are provided in Table S5).

Phylum	Genus	ASV	Mean Abundance (%) [*]	Association Strength (r.g) ⁺	P value
Virginia Coast					
Cyanobacteriota	<i>Cyanobium</i> PCC-6307	ASV019	1.08	0.89	0.001
Pseudomonadota	HIMB11	ASV023	0.90	0.86	0.001
Actinomycetota	PeM15	ASV068	0.43	0.54	0.025
Cyanobacteriota	<i>Synechococcus</i> CC9902	ASV056	0.42	0.76	0.001
Actinomycetota	<i>Microbacteriaceae</i>	ASV092	0.29	0.70	0.004
Cyanobacteriota	<i>Synechococcus</i> CC9902	ASV074	0.27	0.82	0.001
Bacteroidota	<i>Mesoflavibacter</i>	ASV130	0.17	0.48	0.034
Cyanobacteriota	<i>Cyanobium</i> PCC-6307	ASV164	0.15	0.94	0.001
Bacteroidota	<i>Formosa</i>	ASV075	0.14	0.83	0.001
Cyanobacteriota	<i>Cyanobium</i> PCC-6307	ASV176	0.13	0.93	0.001
Delaware Coast Summer					
Pseudomonadota	Comamonadaceae	ASV079	0.24	0.42	0.039
Verrucomicrobiota	Roseibacillus	ASV085	0.24	0.80	0.001
Pseudomonadota	Clade III	ASV071	0.24	0.78	0.001
Pseudomonadota	SAR116 clade	ASV105	0.22	0.62	0.003
Pseudomonadota	OM60(NOR5) clade	ASV107	0.18	0.68	0.001
Pseudomonadota	Litorivicinus	ASV099	0.17	0.70	0.001
Pseudomonadota	SAR92 clade	ASV152	0.15	0.46	0.032
Bacteroidota	NS5 marine group	ASV123	0.15	0.76	0.001
Bacteroidota	NS5 marine group	ASV150	0.15	0.55	0.015
Bacteroidota	NS4 marine group	ASV086	0.13	0.66	0.003
Continental Slope					
Cyanobacteriota	<i>Prochlorococcus</i> MIT9313	ASV003	3.18	0.95	0.001
Cyanobacteriota	<i>Cyanobium</i> PCC-6307	ASV006	2.85	0.81	0.001



SAR324 clade (Marine group B)	SAR324 clade insertae sedis	ASV024	0.86	0.79	0.001
Pseudomonadota	<i>Paracoccaceae</i>	ASV032	0.48	0.90	0.001
Pseudomonadota	SAR116 clade	ASV042	0.40	0.91	0.001
Cyanobacteriota	<i>Synechococcus</i> CC9902	ASV016	0.38	0.87	0.001
Pseudomonadota	Clade Ib	ASV007	0.35	0.76	0.001
Pseudomonadota	SAR116 clade	ASV036	0.26	0.77	0.001
Pseudomonadota	SAR86 clade	ASV043	0.25	0.90	0.001
Pseudomonadota	KI89A clade	ASV063	0.23	0.72	0.001
Delaware Coast Fall					
Pseudomonadota	Clade Ia	ASV002	10.16	0.80	0.001
Pseudomonadota	SAR86 clade	ASV008	1.78	0.71	0.001
Actinomycetota	<i>Candidatus Actinomarina</i>	ASV011	1.42	0.93	0.001
Pseudomonadota	SAR86 clade	ASV014	1.19	0.89	0.001
Bacteroidota	NS5 marine group	ASV017	1.05	0.88	0.001
Bacteroidota	NS5 marine group	ASV025	0.67	0.99	0.001
Pseudomonadota	<i>Candidatus Puniceispirillum</i>	ASV037	0.35	0.84	0.001
Pseudomonadota	SAR86 clade	ASV048	0.28	0.92	0.001
Pseudomonadota	SUP05 cluster	ASV058	0.25	0.94	0.001
Cyanobacteriota	<i>Synechococcus</i> CC9902	ASV015	0.25	0.82	0.001

386 *Mean relative abundance (%) of each ASV calculated across all samples.

387 ⁺Group-equalized point-biserial correlation coefficient (r.g) indicating the strength of association
388 between each ASV and sample stations.

389



390 **Table 4:** Division and genus of the top 10 most abundant protist lineages (ASVs) significantly
 391 associated with each sampling station, with mean abundance, association strength, and P value
 392 (additional significant lineages are provided in Table S6).

Division	Genus	ASV	Mean Abundance (%) [*]	Association Strength (r.g) ⁺	P value
Virginia Coast					
Chlorophyta	<i>Chlorellales_X</i>	ASV117	0.30	0.85	0.001
Alveolata	<i>Dinophyceae</i>	ASV040	0.26	0.89	0.001
Chlorophyta	<i>Picochlorum</i>	ASV101	0.26	0.84	0.001
Stramenopiles	<i>Leptocylindrus</i>	ASV010	0.24	0.81	0.001
Stramenopiles	<i>Guinardia</i>	ASV065	0.23	0.84	0.001
Stramenopiles	<i>Thalassiosiraceae</i>	ASV127	0.21	0.98	0.001
Stramenopiles	<i>Cyclotella</i>	ASV121	0.20	0.90	0.001
Alveolata	Dino-Group-II-Clade-6_X	ASV160	0.18	0.74	0.002
Stramenopiles	<i>Minutocellus</i>	ASV161	0.16	0.92	0.001
Alveolata	Dino-Group-II-Clade-6_X	ASV055	0.16	0.99	0.001
Delaware Coast Summer					
Chlorophyta	<i>Ostreococcus</i>	ASV034	1.86	0.71	0.004
Stramenopiles	MAST-9D	ASV094	1.67	0.89	0.001
Alveolata	<i>Gyrodinium</i>	ASV063	0.77	0.62	0.01
Alveolata	<i>Dinophyceae</i>	ASV116	0.63	0.65	0.008
Alveolata	<i>Gonyaulax</i>	ASV148	0.59	0.63	0.006
Alveolata	<i>Dadayiella</i>	ASV392	0.48	0.87	0.001
Stramenopiles	MAST-4B	ASV141	0.31	0.53	0.025
Alveolata	Dino-Group-II-Clade-3_X	ASV235	0.27	0.53	0.034
Alveolata	<i>Gonyaulax</i>	ASV197	0.27	0.57	0.013
Alveolata	<i>Strombidiidae</i>	ASV523	0.23	0.67	0.002
Continental Slope					
Alveolata	Dino-Group-II-Clade-6_X	ASV012	3.04	0.89	0.001
Alveolata	Dino-Group-I-Clade-5_X	ASV025	2.70	0.97	0.001
Alveolata	Dino-Group-I-Clade-1_X	ASV032	1.03	0.81	0.002
Chlorophyta	<i>Chloropicon</i>	ASV045	0.82	0.91	0.001
Alveolata	Dino-Group-II-Clade-6_X	ASV039	0.81	0.87	0.001
Alveolata	<i>Strombidiidae_X</i>	ASV162	0.60	0.53	0.02
Alveolata	Dino-Group-II-Clade-10-and-11_X	ASV058	0.57	0.83	0.001
Alveolata	Dino-Group-I-Clade-1_X	ASV056	0.56	0.54	0.026
Alveolata	<i>Dinophyceae</i>	ASV064	0.55	0.65	0.006
Chlorophyta	Prasino-Clade-9_XXX	ASV136	0.53	0.86	0.003
Delaware Coast Fall					
Chlorophyta	<i>Ostreococcus</i>	ASV001	16.70	0.77	0.001
Alveolata	<i>Dinophyceae</i>	ASV011	0.91	0.97	0.001
Rhizaria	<i>Acanthometra</i>	ASV018	0.78	0.88	0.001



Stramenopiles	<i>Minidiscus</i>	ASV017	0.60	0.98	0.001
Picozoa	<i>Picomonas</i>	ASV027	0.59	0.92	0.001
Cryptophyta	<i>Plagioselmis</i>	ASV016	0.50	0.66	0.008
Chlorophyta	<i>Micromonas</i>	ASV023	0.47	0.93	0.001
Chlorophyta	<i>Bathycoccus</i>	ASV008	0.46	0.78	0.002
Alveolata	Dino-Group-II-Clade-14_X	ASV038	0.28	0.97	0.001
Stramenopiles	Pelagomonadales clade B1	ASV041	0.28	0.85	0.001

393 *Mean relative abundance (%) of each ASV calculated across all samples.

394 ⁺Group-equalized point-biserial correlation coefficient (r.g) indicating the strength of association
395 between each ASV and sample stations.

396 3.7 Site and Season Associated Microbial Taxa

397 Indicator species analysis also revealed distinct microbial assemblages associated with the
398 different stations across both bacterial (Table 3) and protist (Table 4) communities. The Virginia
399 Coast station was characterized by a highly productive coastal assemblage in both communities.
400 Bacterial indicators were dominated by Cyanobacteria, particularly *Cyanobium* PCC-6307 and
401 *Synechococcus* CC9902 ASVs, alongside heterotrophic taxa including *Formosa*, *Mesoflavibacter*,
402 and *Microbacteriaceae*. The protist community was dominated by diatoms including
403 *Leptocylindrus*, *Guinardia*, *Thalassiosiraceae*, *Cyclotella*, and *Minutocellus*.

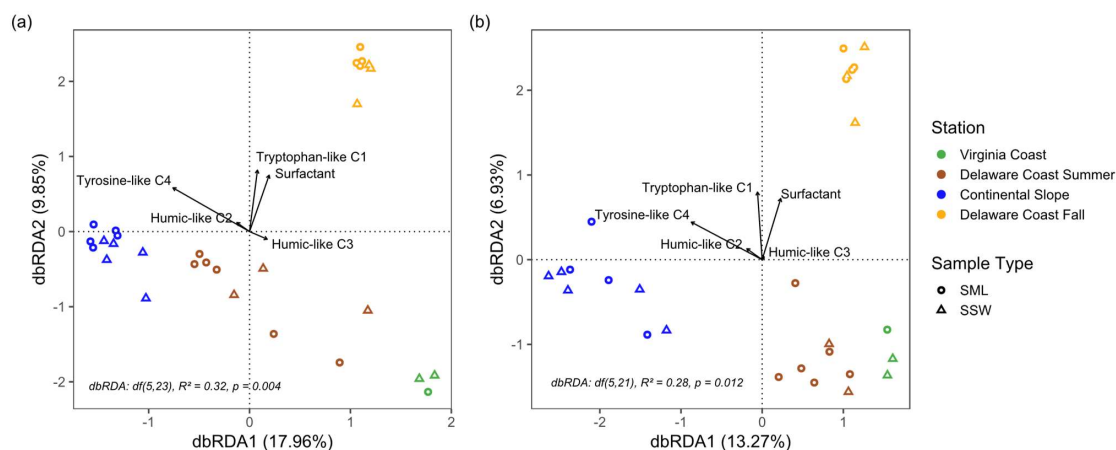
404 The Delaware Coast summer station had more heterotrophic and mixotrophic taxa in both
405 the protist and bacteria communities. Bacteria groups were mainly heterotrophic and included NS4
406 and NS5 marine groups, SAR92 clade, *Litorivincus*, OM60(NOR5) clade, SAR116 clade, and
407 Clade III. The protist community was dominated by dinoflagellates and ciliates, including
408 *Gyrodinium*, *Dinophyceae*, *Dadayiella*, *Gonyaulax*, Dino-Group-II-Clade-3, and *Oligotrichida*,
409 alongside heterotrophic flagellates MAST-4B and MAST-9D.

410 The Delaware Coast fall samples were dominated by phototrophic picoeukaryotic green
411 algae including *Ostreococcus*, *Micromonas*, *Bathycoccus*, and *Plagioselmis*, which corresponds to
412 their highest chlorophyll-a concentration and supports a fall bloom during our sampling. Other



413 abundant protists were small flagellates including *Picomonas* and *Pelagomonadales* clade B1.
 414 Bacteria groups were a combination of both eutrophic and oligotrophic taxa, such as *Candidatus*
 415 *Actinomarina*, *Candidatus Puniceispirillum*, NS5 marine group, SUP05 cluster, and
 416 *Synechococcus* CC9902.

417 The Continental Slope station was distinguished by predominantly oligotrophic taxa.
 418 Bacteria groups included SAR116 clade, SAR86 clade, SAR324 clade, Clade Ib, *Paracoccaceae*,
 419 *Cyanobium* PCC-6307, and *Prochlorococcus* MIT9313. The protist community had multiple
 420 Dino-Group-I and Dino-Group-II clades alongside *Dinophyceae*, *Strombidiidae*, and the
 421 prasinophyte green algae Prasino-Clade-9 and *Chloropicon*.



422

423 **Figure 3:** Distance-based redundancy analysis of (a) bacterial and (b) protist community
 424 composition, constrained by DOM variables across sampling stations. Vectors represent DOM
 425 predictors with direction and length indicating the direction and relative strength of their
 426 relationships with community composition, respectively.

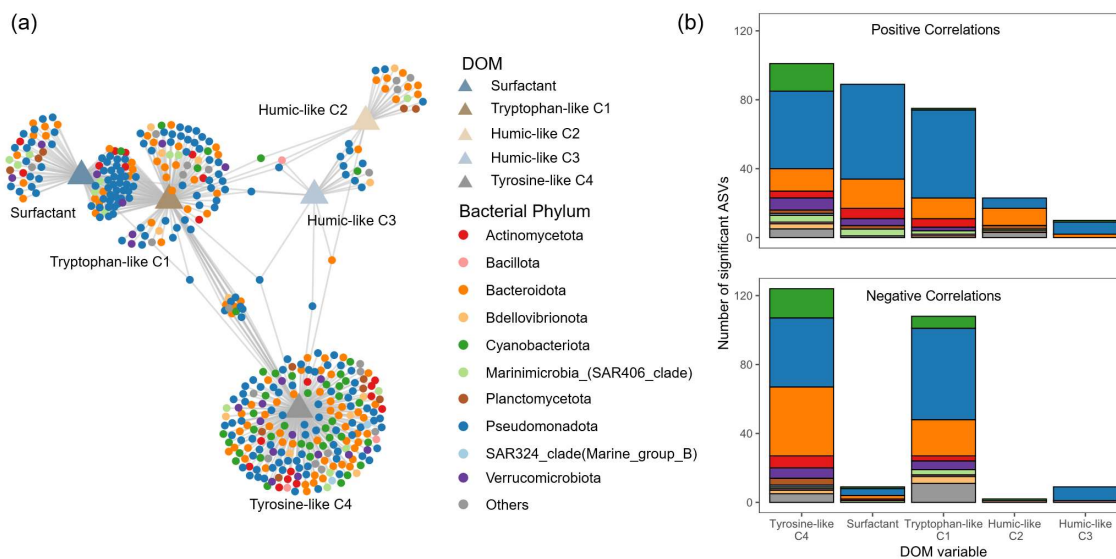
427 3.8 Relationships between Microbial Communities and DOM Composition

428 Surfactant and FDOM concentrations significantly explained the variance in the microbial
 429 composition dataset for both bacteria (dbRDA: $df(5,23)$, $r^2=0.32$, $p=0.004$) and protists (dbRDA:



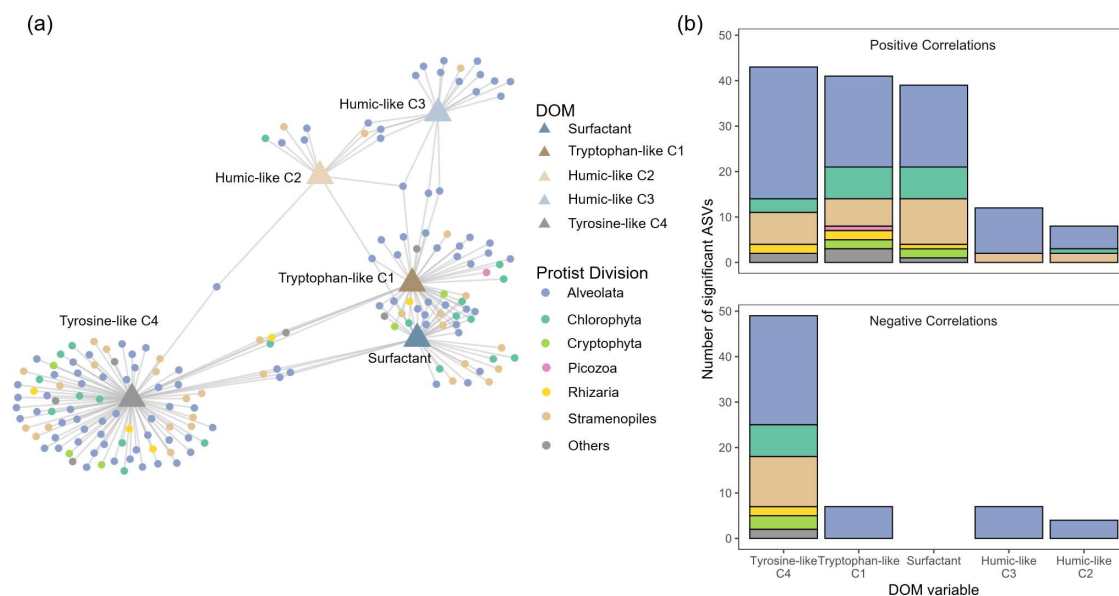
430 $df(5,21)$, $r^2=0.28$, $p=0.012$), suggesting significant relationships between the DOM composition
431 (FDOM component abundance and surfactant concentration) and microbial composition (Figure
432 3). For both bacteria and protists, tyrosine-like C4, tryptophan-like C1, and surfactant
433 concentration explained most of the variations in microbial composition. Tyrosine-like C4 was
434 more associated with the microbial communities of the Continental Slope station, while surfactant
435 concentrations and tryptophan-like C1 were more associated with the fall Delaware Coast
436 microbial communities (Figure 3).

437 The relationships between DOM and microbial communities were further explored
438 through correlation network analysis. The abundance of 448 bacterial (Figure 4; Table S7) and 168
439 protist (Figure 5; Table S8) ASVs were significantly correlated either negatively or positively with
440 FDOM components and surfactant concentrations, forming single interconnected networks
441 (compartments = 1). In both protist and bacterial communities, the highest number of ASVs
442 correlated with tyrosine-like C4 (bacteria: $n = 225$; protists: $n = 92$), followed by tryptophan-like
443 C1 (bacteria: $n = 183$; protists: $n = 48$), and surfactant concentrations (bacteria: $n = 98$; protists: n
444 $= 39$), whereas humic-like components C2 (bacteria, $n = 25$; protists, $n = 12$) and C3 (bacteria: n
445 $= 19$; protists: $n = 19$) correlated with relatively few ASVs. The correlation networks exhibited
446 high modularity (bacteria $Q = 0.529$; protists $Q = 0.558$), where specific groups of ASVs
447 preferentially correlated with specific DOM components rather than interacting broadly across all
448 DOM types.



449

450 **Figure 4:** Correlations between bacterial lineages and DOM composition. (a) Bipartite
 451 correlation network illustrating associations between bacterial ASVs (circles) and DOM
 452 variables (triangles, with associated labels). Edges connect ASVs to the DOM variables with
 453 which they are significantly correlated. (b) Number of bacterial ASVs significantly positively
 454 (upper panel) or negatively (lower panel) correlated with each DOM variable.



455

456 **Figure 5:** Correlations between protist ASVs and DOM composition. (a) Bipartite correlation
 457 network illustrating associations between protist ASVs (circles) and DOM variables (triangles).
 458 Edges connect ASVs to the DOM variables with which they are significantly correlated. (b)
 459 Number of protist ASVs significantly positively (upper panel) or negatively (lower panel)
 460 correlated with each DOM variable.

461 Of the 98 bacterial ASVs correlated with surfactant concentrations, the majority were
 462 positively correlated ($n = 89, 91\%$), with only 9 ASVs (9%) showing negative correlations (Figure
 463 4b). The phylum Pseudomonadota dominated the surfactant associated community, comprising the
 464 largest proportion of positively correlated lineages, including members of the SAR86 and SAR116
 465 clades, *Paracoccaceae*, *Defluviicoccales*, and *Pseudoalteromonas*. Bacteroidota was the second
 466 most prominent phylum, primarily represented by the NS5 and NS9 marine groups. Additional
 467 notable lineages included *Candidatus Actinomarina* and Marinimicrobia (SAR406 clade) (Table
 468 S7).

469 All 39 protist ASVs positively correlated with surfactant concentrations (Figure 5b).
 470 Alveolata was the dominant phylum, driven by diverse dinoflagellate lineages, including



471 unclassified *Dinophyceae*, Dino-Group-II, and Dino-Group-I Clades. Stramenopiles was the
472 second most prominent group, comprising multiple MAST clades (MAST-3A, MAST-3F, MAST-
473 4B, MAST-7B) and *Aureococcus*. Additional taxa included *Teleaulax* (Cryptophyta) and
474 unclassified *Cercozoa* (Rhizaria) (Table S8).

475 Notably, there was high overlap in the bacterial and protist lineages correlating with the
476 surfactant concentrations and the tryptophan-like C1 compared to the other DOM types (Figures
477 4a and 5a). 62 bacterial ASVs (63% of surfactant associated bacterial ASVs) and 24 protist ASVs
478 (62% of surfactant associated protist ASVs) correlated with both surfactant concentrations and
479 tryptophan-like C1 abundance, respectively, supporting the co-association between surfactant
480 concentrations and tryptophan-like C1. In contrast, the overlap between surfactant concentrations
481 and all other FDOM components, tyrosine-like C4 and humic-like C2 and C3 was markedly lower,
482 with shared ASVs representing less than 5% of surfactant associated ASVs in both bacterial and
483 protist networks.

484 The ASVs positively correlated with both surfactant and tryptophan-like C1 comprised a
485 diverse assemblage of phototrophic, phagotrophic, and parasitic protists, along with oligotrophic
486 and copiotrophic bacteria, most of which were abundant during the fall sampling period.
487 Phototrophs included *Ostreococcus*, *Micromonas*, *Bathycoccus*, *Pseudoscurfieldia*, *Aureococcus*,
488 and the diatom *Minidiscus*. Phagotrophic protists included MAST-7B, *Cercozoa*, and *Telonemia*,
489 while parasitic lineages were dominated by multiple Dino-Group-II and Dino-Group-I clades.
490 Oligotrophic bacteria included SAR86, *Candidatus Actinomarina*, *Candidatus Puniceispirillum*,
491 *Puniceispirillales*, AEGEAN-169, and *Marinimicrobia*, whereas copiotrophic taxa included the
492 NS5 marine group, *Pseudoalteromonas*, *Pseudohongiella*, *Porticoccus*, *Haliaceae*,
493 *Ectothiorhodospiraceae*, *Paracoccaceae*, and *Defluviicoccales*. Together, these groups reflect



494 complex trophic interactions associated with the accumulation of surfactants and tryptophan-like
495 C1.

496 **4 Discussion**

497 **4.1 FDOM Supports the Biological Source of Marine Surfactants**

498 Surfactant concentrations showed a significant positive correlation with tryptophan-like
499 FDOM (Peak T) (Figure S1), consistent with previous reports of positive correlations between
500 tryptophan-like FDOM and surfactant-like DOM compositions, including the abundance of
501 unsaturated aliphatic, peptide-like, and sulfur-rich FTICR-MS-derived molecular formulas
502 enriched in the SML (Coffey et al., 2025). Tryptophan-like FDOM is a well-established indicator
503 of freshly produced organic matter in marine waters (Coble, 1996, 2007). It has been shown to
504 correlate strongly with total dissolved amino acid concentrations and serves as a more reliable
505 tracer of recent autochthonous production than tyrosine-like FDOM (Peak B), which has a weaker
506 correlation with total dissolved amino acids (Yamashita et al., 2015). It is produced by both
507 photosynthetic and non-photosynthetic microorganisms and is associated with general microbial
508 activity (Maie et al., 2007; Hudson et al., 2008; Williams et al., 2010; Fox et al., 2017; Devresse
509 et al., 2023). Therefore, its correlation with bulk surfactant concentrations supports previous
510 findings that biogenic processes are the primary source of marine surfactant production
511 (Gašparović and Čosović, 2003; Gašparović et al., 2007; Frka et al., 2009; Wurl et al., 2011) and
512 is consistent with observations by Barthelmeß and Engel (2022), who reported elevated surfactant
513 concentrations during periods of high lability DOM concentrations (e.g., glucose and amino acids).

514 In addition, surfactant concentrations were negatively correlated with terrestrial humic-like
515 FDOM, suggesting that samples with higher contributions of terrestrially derived DOM had lower



516 surfactant concentrations. This reinforces the idea that autochthonous rather than allochthonous
517 organic matter is the dominant contributor to the marine surfactant pool.

518 **4.2 SML Associated Taxa are Distinct from SSW**

519 The microbial communities in both SML and SSW were generally dominated by the
520 bacteria phyla Pseudomonadota, Cyanobacteriota, Bacteroidota, and Actinomycetota, as well as
521 the protist divisions Alveolata, Chlorophyta, and Stramenopiles, which represent typical surface
522 seawater communities (Li et al., 2018; Lang-Yona et al., 2022; Cohen et al., 2024) and SML
523 communities (Cunliffe et al., 2011; Taylor and Cunliffe, 2014; Rahlff et al., 2021; Zäncker et al.,
524 2021; Tastassa et al., 2025). The majority of microbial lineages were similarly distributed between
525 the SML and SSW, consistent with previous studies (Zäncker et al., 2021). However, some specific
526 lineages were significantly associated with either the SML or SSW and will provide further
527 understanding of the factors that influence microbial enrichment and biogeochemical processes in
528 the SML.

529 The SML associated bacterial lineages were primarily small-sized photoheterotrophs,
530 including SAR86 and SAR116, which have been previously reported to be in the SML (Rahlff et
531 al., 2021). Additionally, *Candidatus Actinomarina*, *Candidatus Puniceispirillum*, and the
532 AEGEAN-169 marine group, which represent newly identified SML associated bacterial lineages,
533 were observed. These bacterial lineages are generally characterized by streamlined genomes that
534 enable efficient resource utilization and adaptation to oligotrophic conditions, as has been observed
535 in previous work (Swan et al., 2013; Brown et al., 2014; Oggerin et al., 2024). They typically
536 exhibit specialized light adaptations, such as the possession of proteorhodopsin (e.g., SAR86,
537 SAR116 and *Candidatus Puniceispirillum*) and MACrhodopsin (e.g., *Candidatus Actinomarina*),
538 which enable them to utilize sunlight for energy to sustain basal metabolism and support biomass



539 synthesis or growth (Palovaara et al., 2014; Gómez-Consarnau et al., 2019; Oggerin et al., 2024).
540 They also possess metabolic adaptations for sulfur redox cycling (Van Mooy et al., 2006; Grote et
541 al., 2012; Ramfelt et al., 2024), which may explain the abundance of sulfur-containing compounds
542 in the SML in previous work (Lechtenfeld et al., 2013; Liu et al., 2023; Coffey et al., 2025; Birt et
543 al., 2026). Additionally, their small cell sizes may enhance attachment to buoyant organic
544 aggregates, aiding their accumulation in the SML through buoyancy effects (Zäncker et al., 2018).
545 In contrast, the SSW associated bacterial lineages included *Caulobacter*, *Cupriavidus*,
546 *Alteromonas*, *Comamonadaceae* and *Mesoflavibacter*, which are characterized by heterotrophic
547 lifestyles. These taxa generally lack prominent light-harvesting adaptations, such as
548 proteorhodopsin and tend to possess larger genomes that enable the degradation of complex
549 organic matter (Asker et al., 2007; Poehlein et al., 2011; López-Pérez et al., 2012; Wilhelm, 2018).
550 This metabolic capability is likely advantageous in the SSW, where more aromatic and humified
551 DOM is present compared to the SML.

552 Phytoplankton are known to exhibit special light adaptations, such as possession of
553 photoprotective proteins or vertical migration in the water column to receive optimal light for
554 photosynthesis (Lichtenberg et al., 2020; Becker et al., 2021; Salonen et al., 2024). Most
555 phytoplankton were not significantly associated with only the SML or SSW, suggesting frequent
556 movement between the two layers, consistent with their migratory behavior (Lichtenberg et al.,
557 2020; Salonen et al., 2024) and the fact that samples were collected across different times of the
558 day with different sunlight intensities. However, the green alga *Ostreococcus* was consistently
559 enriched in the SML, which may be attributed to its efficient photosystem I antenna adjustment
560 system that enables acclimation to high light intensities (Ishii et al., 2023). Similar to the dominant
561 SML associated bacterial lineages, *Ostreococcus* is small in size and adapted to survive under low



562 nutrient conditions (Martin et al., 2020). Other prominent SML associated protists were
563 dinoflagellate parasites (Syndiniales), which have previously been reported to dominate both the
564 SML and SSW taxa (Zäncker et al., 2021). The Syndiniales are intracellular parasites which infect
565 a broad range of protist and metazoan hosts (Siano et al., 2011; Christaki et al., 2023). Their
566 presence in the SML could be due to the enrichment of their hosts such as other protists like
567 *Ostreococcus* and *Cryomonadida* that were enriched in the SML or zooplankton, which have also
568 been previously observed to be enriched in the SML (Zäncker et al., 2021). Syndiniales have
569 complex life cycles involving intracellular trophont stages that lyse hosts and release numerous
570 short-lived dinospores (Siano et al., 2011; Christaki et al., 2023). This lytic process may also
571 contribute to organic matter enrichment in the SML through the release of host cell contents. The
572 SSW associated protist lineages, in contrast, were relatively large in size and typically mixotrophic
573 dinoflagellates and ciliates that can undergo photosynthesis or switch to phagotrophy during light
574 or nutrient stress (Li et al., 2000; Jeong et al., 2005; Stoecker et al., 2017).

575 **4.3 Candidate Surfactant and Tryptophan-like FDOM Associated Microbial Communities**

576 Our sampling across diverse hydrographic regions captured variations in bacterial and
577 protist compositions along with surfactant and FDOM concentrations, which allowed us to identify
578 biomarkers and microorganisms associated with surfactants. The microbial compositional
579 differences across regions reflected a classic terrestrial-to-marine gradient (Cohen et al., 2024;
580 Ruff et al., 2024). The coastal stations (Delaware Coast and Virginia Coast) were dominated by
581 microbes typically associated with coastal and eutrophic ecosystems, whereas the Continental
582 Slope was mainly dominated by oligotrophic microbes. A phytoplankton bloom, dominated by the
583 picoeukaryotic green algae *Ostreococcus*, *Bathycoccus*, and *Micromonas*, was also observed
584 during fall sampling. Surfactant and tryptophan-like FDOM concentrations were highest during



585 the fall bloom, consistent with the increased production and release of freshly produced organic
586 matter and surfactants during bloom events (Barthelmeß and Engel, 2022) and suggests a greater
587 temporal influence on surfactant production compared to spatial influences.

588 Several microbial lineages (bacteria = 89; protist = 39) were positively correlated with
589 surfactant concentrations, and a majority of these (bacteria = 63%; protist = 62%) also showed
590 positive correlations with tryptophan-like FDOM, further supporting the co-occurrence of
591 surfactants and tryptophan-like FDOM. These lineages represent key candidates as surfactant
592 producers or indicators. Notable taxa include the small-sized phytoplankton *Ostreococcus*,
593 *Micromonas*, *Bathycoccus*, *Pseudoscourfieldia*, and *Aureococcus*, as well as the diatom
594 *Minidiscus*, which were dominant during the fall bloom. While nanophytoplankton abundance has
595 been shown to be tightly coupled with surfactant concentrations (Barthelmeß and Engel, 2022),
596 our data provide new insight into the specific pico- to nano-phytoplankton taxa that may drive this
597 relationship. Small photoautotrophs such as *Ostreococcus* are known to dominate coastal waters,
598 where they shape overall microbial community metabolic profiles (Aylward et al., 2015). With the
599 increasing frequency and spatial extent of phytoplankton blooms documented in recent decades,
600 particularly in coastal regions (Dai et al., 2023), their abundance is likely to increase along with
601 surfactant production and accumulation in the SML. Previous studies using culture and bloom-
602 induced mesocosm experiments have linked larger phytoplankton such as *Emiliana huxleyi*,
603 *Cylindrotheca closterium*, and *Skeletonema* (Zutic et al., 1981; Bibi et al., 2025; Flores et al., 2025)
604 to increases in surfactant concentrations. These taxa are mostly abundant during high nutrient and
605 optimal light conditions like spring blooms, which were not captured in the present study and
606 support a strong temporal influence on microbial composition and surfactant production.



607 Heterotrophic bacterial groups, including the NS5 marine group, *Pseudoalteromonas*,
608 *Pseudohongiella*, *Porticoccus*, *Haliaceae*, *Ectothiorhodospiraceae*, *Paracoccaceae*, and
609 *Defluviicoccales*, were also positively correlated with surfactant and tryptophan-like FDOM
610 concentrations. While their association with surfactants may suggest a preference for degrading
611 surfactant-like compounds, these heterotrophic bacteria could also produce surfactants. For
612 example, *Paracoccaceae* and *Pseudoalteromonas* are known to produce biosurfactants that enable
613 them to metabolize hydrocarbon-rich organic matter (Antoniou et al., 2015; Morales-Guzmán et
614 al., 2021). These bacterial groups may also contribute to surfactant production through metabolic
615 interactions with phytoplankton, as some bacteria produce certain secondary organic compounds
616 only in the presence of green algae (Sousoni, 2018; Chhun et al., 2021). Notably, oligotrophic-
617 adapted bacterial groups that were more abundant in the SML, including SAR86, *Candidatus*
618 *Actinomarina*, *Candidatus Puniceispirillum*, *Puniceispirillales*, and AEGEAN-169, were also
619 positively correlated with surfactant and tryptophan-like FDOM concentrations. Their consistent
620 association with both the SML and surfactant concentrations, combined with their ubiquity in the
621 global ocean, suggests that these groups could represent promising candidates for tracking
622 surfactant production across the global ocean.

623 Additional surfactant associated taxa were phagotrophic protists, including MAST-7B,
624 *Cercozoa*, and *Telonemia*, as well as parasitic dinoflagellates of Dino-Group-I and Dino-Group-II
625 clades. These associations point to additional and relatively underexplored surfactant production
626 mechanisms. Phagotrophic protists are active grazers of bacteria and small phytoplankton, and
627 their feeding involves cell lysis, which disrupts microbial membranes and releases intracellular
628 material into the DOM pool. This material includes membrane lipids, amino acids, and other
629 amphiphilic compounds with surface-active properties (Kujawinski et al., 2002). Parasitic



630 dinoflagellates may contribute through similar processes, as infection and host cell lysis also
631 release intracellular contents. These lysis-driven mechanisms of surfactant production alongside
632 viral lysis, which likewise releases cellular contents, may play important roles in surfactant release
633 and in predicting the timing of surfactant impacts on air-sea processes.

634 **4.4 Implications for Understanding Surfactants in the Ocean and Future Work**

635 Overall, our results highlight the diversity of microbial processes in the SML and the
636 potential roles of different microbial communities in regulating surfactant composition and, by
637 extension, air-sea interactions. In general, SML associated microbes, comprising both bacterial
638 and protist taxa, are small in size and adapted to high-light and low-nutrient conditions compared
639 to the SSW associated microbes, which tend to be larger and exhibit more flexible trophic
640 strategies. These contrasting lifestyles suggest that the SML was relatively nutrient limited under
641 our sampling conditions, or that its harsh physicochemical conditions favor microorganisms with
642 stress tolerant and resource efficient lifestyles (Carlucci et al., 1985; Agogu e et al., 2005). The
643 smaller cell sizes of SML associated taxa may also promote their physical accumulation at the sea
644 surface through buoyancy effects.

645 The composition of SML associated microbial communities has direct implications for
646 organic matter and surfactant production at the air-sea interface. The enrichment of the green algae
647 *Ostreococcus* in the SML points to active primary production and autochthonous synthesis of
648 organic matter, consistent with observations of unique photosynthetic biomarker lipids in the SML
649 (Birt et al., 2026). The enriched photoheterotrophic bacteria may further contribute to organic
650 matter production through light-enhanced anoxygenic CO₂ fixation, whereby inorganic CO₂ is
651 assimilated into biomass (Palovaara et al., 2014). At the same time, these bacteria may also drive
652 biotic degradation of organic matter in the SML (Birt et al., 2026).



653 The nature of nutrient limitation in the SML warrants further investigation. Nitrate plus
654 nitrite concentrations were higher in the SML than in the SSW (Table S1), suggesting that nitrogen
655 is not the primary limiting nutrient and instead pointing toward phosphorus limitation. Under
656 phosphorus limitation, microorganisms are known to substitute phosphorus-containing membrane
657 lipids with sulfolipids and betaine lipids, resulting in organic matter enriched in sulfur- and
658 nitrogen-containing compounds (Benning et al., 1995; Van Mooy et al., 2006). This is consistent
659 with the abundance of such compounds previously reported in the SML (Lechtenfeld et al., 2013;
660 Coffey et al., 2025; Birt et al., 2026) and suggests that phosphorus limitation may partly shape the
661 molecular composition of surfactants and DOM accumulating in the SML.

662 Our study identifies microbial groups significantly correlated with surfactant
663 concentrations, representing candidate surfactant associated microbial communities. While
664 correlations do not imply causation, these groups of microbes will serve as a starting point for
665 critical screening of marine surfactant producers or biomarkers. The diversity of the surfactant
666 associated microbial candidates, spanning both photosynthetic and non-photosynthetic lineages,
667 suggests that surfactant concentrations in marine waters may reflect a broad range of microbial
668 activities rather than a single dominant process. Notably, cell lysis by parasitic and phagotrophic
669 protists appears to be an important and previously underexplored potential determinant of
670 surfactant concentrations. If these lytic processes are indeed important sources of surfactants via
671 the release of biological lipids and amino acids that are excellent potential surfactant compounds
672 due to their amphiphilic properties, relationships between viral abundances and lytic processes
673 warrant further investigation.

674 The biological diversity of surfactant associated microbial candidates may explain why
675 surfactant concentrations do not correlate well with chlorophyll-a ($r = 0.09$, $df = 29$, $p = 0.62$),



676 consistent with previous observations (Pereira et al., 2018; Frossard et al., 2019). In contrast,
677 tryptophan-like FDOM showed a stronger correlation with surfactant concentrations ($r = 0.68$, df
678 $= 30$, $p < 0.0001$) and may serve as a better proxy for estimating surfactant concentrations. Unlike
679 chlorophyll-a, tryptophan-like FDOM is produced by both photosynthetic and non-photosynthetic
680 microbial communities and reflects general microbial metabolic activity rather than photosynthesis
681 alone (Maie et al., 2007; Hudson et al., 2008; Williams et al., 2010; Fox et al., 2017; Devresse et
682 al., 2023), making it better suited to capture the diverse biological sources of marine surfactants.
683 Additionally, while distance-based redundancy analysis revealed significant relationships among
684 surfactant concentrations, FDOM composition, and microbial community composition, the
685 relatively low variance explained ($\sim 30\%$) indicates that additional factors not captured in this study
686 including photodegradation, vertical mixing, and bloom dynamics are also significant in
687 determining surfactants, FDOM or microbial composition.

688 Targeted laboratory experiments are needed to validate the candidate surfactant producing
689 taxa and quantify their impact on air-sea processes. We recommend combining targeted laboratory
690 incubations with integrative omics, including metabolomics, metagenomics, and proteomics to (i)
691 validate candidate microbial surfactant producers, (ii) identify the molecular identities of
692 surfactants produced, and (iii) quantify their functional impacts on surface tension and gas
693 exchange. This study did not capture all stages of the fall phytoplankton bloom cycle, which could
694 be a future topic of study. Bloom progression from autotrophic growth through decline and into
695 heterotrophic degradation, as well as protist and viral lysis, is likely important for understanding
696 surfactant production dynamics (Flores et al., 2025). Characterizing surfactant concentrations and
697 composition across a naturally occurring bloom life cycle therefore represents an important
698 direction for future work.



699 Finally, this study demonstrates that combining microbial sequencing with surfactant
700 concentration measurements is a promising approach for identifying microbial lineages
701 influencing surfactant concentrations. Predicting the spatiotemporal distributions of these
702 microbial groups can improve understanding of surfactant variability and their consequences for
703 air-sea exchange processes. Furthermore, advances in remote sensing and satellite imaging of
704 marine microbes (IOCCG, 2014; Mouw et al., 2017), may enable the development of microbial-
705 based proxies to improve parameterization of gas transfer velocities and enhance predictions of
706 regional to global fluxes of climate-active gases.

707 **Code and Data Availability**

708 All code and datasets used in this study have been deposited on
709 <https://github.com/FEdufia/SOAPI1and2-MicrobesAndSurfactants>

710 **Supplement Link:**

711 **Acknowledgements**

712 This work was primarily supported by the National Science Foundation (NSF) through
713 awards OCE-2123368 to the University of Georgia and OCE-2123402 to the University of
714 Delaware. The authors are grateful to the captain, marine operations staff, and crew of the *R/V*
715 *Hugh R. Sharp* for their support with cruise operations and sample collection. The authors also
716 thank Dr. Tret Burdette, Dr. Rachel Bramblett, Abigail Sanders, and Ariana Deegan from the
717 University of Georgia; Dr. Alina Ebling, Dr. Tia Ouyang, Chris Kelly, Pam Edris, Ava Grove,
718 Audrey Tong, Nicole Gutkowski, and Zeal Goolesby from the University of Delaware; and Dr.
719 Siddhartha Mitra, Zachary Shepherd, and Michael Zigah from East Carolina University for their
720 assistance with sample collection and processing.

721 **Author Contributions**

722 FE Agblemanyo: Investigation, methodology, data curation, formal analysis, validation,
723 visualization, writing – original draft, writing – review & editing.



724 D Ammer: Investigation, methodology, data curation, validation, writing – review & editing.

725 AE Birt: Investigation, methodology, data curation, validation, writing – review & editing.

726 MR Bowen: Investigation, methodology, validation, writing – review & editing.

727 JF Biddle: Investigation, methodology, validation, writing – review & editing.

728 AA Frossard: Conceptualization, investigation, methodology, validation, writing – review &
729 editing, supervision, funding acquisition.

730 AS Wozniak: Conceptualization, investigation, methodology, validation, writing – original draft,
731 writing – review & editing, supervision, funding acquisition.

732 **Competing Interests**

733 The authors declare that they have no conflict of interest.

734



735 References

- 736 Agblemanyo, F. E., Frossard, A. A., Wozniak, A. S., Ammer, D., and Birt, A. E.: The Rosette-Based
737 Glass Plate (RGP) Sampler: A Cost-Effective Technique for High-Volume, Low-Thickness
738 Sea Surface Microlayer Collection., *Limnol. Oceanogr.:Methods* “in review”, 2026.
- 739 Agogué, H., Joux, F., Obernosterer, I., and Lebaron, P.: Resistance of Marine Bacterioneuston to
740 Solar Radiation, *Appl Environ Microb*, 71, 5282-5289, doi:10.1128/AEM.71.9.5282-
741 5289.2005, 2005.
- 742 Aminot, A. and Rey, F.: Standard procedure for the determination of chlorophyll a by spectroscopic
743 methods, *International Council for the Exploration of the Sea*, 112, 2000.
- 744 Antoniou, E., Fodelianakis, S., Korkakaki, E., and Kalogerakis, N.: Biosurfactant production from
745 marine hydrocarbon-degrading consortia and pure bacterial strains using crude oil as
746 carbon source, *Front Microbiol*, Volume 6 - 2015, 10.3389/fmicb.2015.00274, 2015.
- 747 Asker, D., Beppu, T., and Ueda, K.: Mesoflavibacter zeaxanthinifaciens gen. nov., sp. nov., a novel
748 zeaxanthin-producing marine bacterium of the family Flavobacteriaceae, *Systematic and
749 Applied Microbiology*, 30, 291-296, <https://doi.org/10.1016/j.syapm.2006.12.003>, 2007.
- 750 Aylward, F. O., Eppley, J. M., Smith, J. M., Chavez, F. P., Scholin, C. A., and DeLong, E. F.:
751 Microbial community transcriptional networks are conserved in three domains at ocean
752 basin scales, *Proceedings of the National Academy of Sciences*, 112, 5443-5448,
753 doi:10.1073/pnas.1502883112, 2015.
- 754 Barthelmeß, T. and Engel, A.: How biogenic polymers control surfactant dynamics in the surface
755 microlayer: insights from a coastal Baltic Sea study, *Biogeosciences*, 19, 4965-4992,
756 10.5194/bg-19-4965-2022, 2022.
- 757 Becker, K. W., Harke, M. J., Mende, D. R., Muratore, D., Weitz, J. S., DeLong, E. F., Dyhrman, S.
758 T., and Van Mooy, B. A. S.: Combined pigment and metatranscriptomic analysis reveals
759 highly synchronized diel patterns of phenotypic light response across domains in the open
760 oligotrophic ocean, *The ISME Journal*, 15, 520-533, 10.1038/s41396-020-00793-x, 2021.
- 761 Benning, C., Huang, Z. H., and Gage, D. A.: Accumulation of a Novel Glycolipid and a Betaine
762 Lipid in Cells of *Rhodobacter sphaeroides* Grown under Phosphate Limitation, *Archives
763 of Biochemistry and Biophysics*, 317, 103-111, <https://doi.org/10.1006/abbi.1995.1141>,
764 1995.
- 765 Bibi, R., Ribas-Ribas, M., Jaeger, L., Lehnert, C., Gassen, L., Cortés-Espinoza, E. F.,
766 Wollschläger, J., Thölen, C., Waska, H., Zöbelein, J., Brinkhoff, T., Athale, I., Röttgers, R.,
767 Novak, M., Engel, A., Barthelmeß, T., Karnatz, J., Reinthaler, T., Spriahailo, D., Friedrichs,
768 G., Schäfer, F. A., and Wurl, O.: Biogeochemical dynamics of the sea-surface microlayer
769 in a multidisciplinary mesocosm study, *Biogeosciences*, 22, 7563-7589, 10.5194/bg-22-
770 7563-2025, 2025.
- 771 Birt, A. E., Ammer, D., Agblemanyo, F. E., Wozniak, A. S., and Frossard, A. A.: Analysis of lipid
772 composition using liquid chromatography and high-resolution mass spectrometry for
773 understanding surfactant properties in seawater and the sea surface microlayer *ACS Earth
774 and Space Chemistry*, "Under review", 2026.
- 775 Bramblett, R. L. and Frossard, A. A.: Evaluating the extraction and quantification of marine
776 surfactants from seawater through solid phase extraction and subsequent colorimetric
777 analyses, *ACS Environmental Science and Technology - Water*,
778 10.1021/acsestwater.4c00497, 2024.



- 779 Brown, M. V., Ostrowski, M., Grzymski, J. J., and Lauro, F. M.: A trait based perspective on the
780 biogeography of common and abundant marine bacterioplankton clades, *Marine*
781 *Genomics*, 15, 17-28, <https://doi.org/10.1016/j.margen.2014.03.002>, 2014.
- 782 Burdette, T. C. and Frossard, A. A.: Characterization of seawater and aerosol particle surfactants
783 using solid phase extraction and mass spectrometry, *Journal of Environmental Sciences*,
784 2021.
- 785 Burdette, T. C., Bramblett, R. L., Deegan, A. M., Coffey, N. R., Wozniak, A. S., and Frossard, A.
786 A.: Organic Signatures of Surfactants and Organic Molecules in Surface Microlayer and
787 Subsurface Water of Delaware Bay, *Acs Earth and Space Chemistry*, 6, 2929-2943,
788 10.1021/acsearthspacechem.2c00220, 2022.
- 789 Čanković, M., Dutour-Sikirić, M., Radić, I. D., and Ciglencečki, I.: Bacterioneuston and
790 Bacterioplankton Structure and Abundance in Two Trophically Distinct Marine
791 Environments — a Marine Lake and the Adjacent Coastal Site on the Adriatic Sea,
792 *Microbial Ecology*, 84, 996-1010, 2022.
- 793 Caporaso, J. G., Lauber, C. L., Walters, W. A., Berg-Lyons, D., Huntley, J., Fierer, N., Owens, S.
794 M., Betley, J., Fraser, L., Bauer, M., Gormley, N., Gilbert, J. A., Smith, G., and Knight, R.:
795 Ultra-high-throughput microbial community analysis on the Illumina HiSeq and MiSeq
796 platforms, *The ISME Journal*, 6, 1621-1624, 10.1038/ismej.2012.8, 2012.
- 797 Carlucci, A. F., Craven, D. B., and Henrichs, S. M.: Surface-film microheterotrophs: amino acid
798 metabolism and solar radiation effects on their activities, *Marine Biology*, 85, 13-22,
799 10.1007/BF00396410, 1985.
- 800 Chen, J., Li, H., Zhao, T., Chen, K., Chen, M.-H., Sun, Z., Xu, W., Maas, K., Lester, B. M., and
801 Cong, X. S.: The Impact of Early Life Experiences and Gut Microbiota on Neurobehavioral
802 Development in Preterm Infants: A Longitudinal Cohort Study, *Microorganisms*, 11, 814,
803 2023.
- 804 Chhun, A., Sousoni, D., Aguiló-Ferretjans, M. d. M., Song, L., Corre, C., and Christie-Oleza, J.
805 A.: Phytoplankton trigger the production of cryptic metabolites in the marine
806 actinobacterium *Salinispora tropica*, *Microbial Biotechnology*, 14, 291-306,
807 <https://doi.org/10.1111/1751-7915.13722>, 2021.
- 808 Christaki, U., Skouroliakou, D.-I., and Jardillier, L.: Interannual dynamics of putative parasites
809 (Syndiniales Group II) in a coastal ecosystem, *Environmental Microbiology*, 25, 1314-
810 1328, <https://doi.org/10.1111/1462-2920.16358>, 2023.
- 811 Coble, P. G.: Characterization of marine and terrestrial DOM in seawater using excitation-emission
812 matrix spectroscopy, *Marine Chemistry*, 51, 325-346, [https://doi.org/10.1016/0304-
813 4203\(95\)00062-3](https://doi.org/10.1016/0304-4203(95)00062-3), 1996.
- 814 Coble, P. G.: *Marine Optical Biogeochemistry: The Chemistry of Ocean Color*, *Chemical*
815 *Reviews*, 107, 402-418, 10.1021/cr050350+, 2007.
- 816 Cochran, R. E., Laskina, O., Jayarathne, T., Laskin, A., Laskin, J., Lin, P., Sultana, C., Lee, C.,
817 Moore, K. A., Cappa, C. D., Bertram, T. H., Prather, K. A., Grassian, V. H., and Stone, E.
818 A.: Analysis of Organic Anionic Surfactants in Fine and Coarse Fractions of Freshly
819 Emitted Sea Spray Aerosol, *Environmental Science & Technology*, 50, 2477-2486,
820 10.1021/acs.est.5b04053, 2016.
- 821 Coffey, N. R., Agblemany, F. E., McKenna, A. M., and Wozniak, A. S.: Unsaturated aliphatic and
822 sulfur-containing organic matter as surfactants in the surface microlayer, *Marine*
823 *Chemistry*, 272, 104547, <https://doi.org/10.1016/j.marchem.2025.104547>, 2025.



- 824 Cohen, N. R., Krinos, A. I., Kell, R. M., Chmiel, R. J., Moran, D. M., McIlvin, M. R., Lopez, P.
825 Z., Barth, A. J., Stone, J. P., Alanis, B. A., Chan, E. W., Breier, J. A., Jakuba, M. V., Johnson,
826 R., Alexander, H., and Saito, M. A.: Microeukaryote metabolism across the western North
827 Atlantic Ocean revealed through autonomous underwater profiling, *Nature*
828 *Communications*, 15, 7325, 10.1038/s41467-024-51583-4, 2024.
- 829 Csárdi, G. and Nepusz, T.: The igraph software package for complex network research,
830 *InterJournal, Complex Systems*, 1695, 2006.
- 831 Cunliffe, M., Upstill-Goddard, R. C., and Murrell, J. C.: Microbiology of aquatic surface
832 microlayers, *FEMS Microbiology Reviews*, 35, 233-246, [https://doi.org/10.1111/j.1574-](https://doi.org/10.1111/j.1574-6976.2010.00246.x)
833 [6976.2010.00246.x](https://doi.org/10.1111/j.1574-6976.2010.00246.x), 2011.
- 834 Cunliffe, M., Engel, A., Frka, S., Gašparović, B., Guitart, C., Murrell, J. C., Salter, M., Stolle, C.,
835 Upstill-Goddard, R., and Wurl, O.: Sea surface microlayers: A unified physicochemical and
836 biological perspective of the air–ocean interface, *Progress in Oceanography*, 109, 104-116,
837 <https://doi.org/10.1016/j.pocean.2012.08.004>, 2013.
- 838 Dai, Y., Yang, S., Zhao, D., Hu, C., Xu, W., Anderson, D. M., Li, Y., Song, X.-P., Boyce, D. G.,
839 Gibson, L., Zheng, C., and Feng, L.: Coastal phytoplankton blooms expand and intensify
840 in the 21st century, *Nature*, 615, 280-284, 10.1038/s41586-023-05760-y, 2023.
- 841 De Cáceres, M. and Legendre, P.: Associations between species and groups of sites: indices and
842 statistical inference, *Ecology*, 90, 3566-3574, 10.1890/08-1823.1, 2009.
- 843 Devresse, Q., Becker, K. W., Dilmahamod, A. F., Ortega-Retuerta, E., and Engel, A.: Dissolved
844 Organic Matter Fluorescence as a Tracer of Upwelling and Microbial Activities in Two
845 Cyclonic Eddies in the Eastern Tropical North Atlantic, *Journal of Geophysical Research:*
846 *Oceans*, 128, e2023JC019821, <https://doi.org/10.1029/2023JC019821>, 2023.
- 847 Dormann, C. F., Fründ, J., Blüthgen, N., and Gruber, B.: Indices, graphs and null models: analyzing
848 bipartite ecological networks, *The Open Ecology Journal*, 2, 7-24, 2009.
- 849 Ebling, A. M. and Landing, W. M.: Sampling and analysis of the sea surface microlayer for
850 dissolved and particulate trace elements, *Marine Chemistry*, 177, 134-142,
851 10.1016/j.marchem.2015.03.012, 2015.
- 852 El Haber, M., Gérard, V., Kleinheins, J., Ferronato, C., and Nozière, B.: Measuring the Surface
853 Tension of Atmospheric Particles and Relevant Mixtures to Better Understand Key
854 Atmospheric Processes, *Chemical Reviews*, 124, 10924-10963,
855 10.1021/acs.chemrev.4c00173, 2024.
- 856 Emery, R. M., Welch, E. B., and Christman, R. F.: The Total Organic Carbon Analyzer and Its
857 Application to Water Research, *Journal (Water Pollution Control Federation)*, 43, 1834-
858 1844, 1971.
- 859 Flores, J. M., Trainic, M., Schatz, D., Koren, I., and Vardi, A.: Diurnal Emissions of Sea Spray
860 Aerosols in Algal Blooms, *Environmental Science & Technology*, 59, 24463-24472,
861 10.1021/acs.est.5c12650, 2025.
- 862 Fox, B. G., Thorn, R. M. S., Anesio, A. M., and Reynolds, D. M.: The in situ bacterial production
863 of fluorescent organic matter; an investigation at a species level, *Water Research*, 125, 350-
864 359, 10.1016/j.watres.2017.08.040, 2017.
- 865 Frew, N. M., Nelson, R. K., and Johnson, C. G.: Sea slicks: variability in chemical composition
866 and surface elasticity, in: *Marine Surface Films*, edited by: Gade, M., Huhnerfuss, H., and
867 Korenowski, G. M., Springer, Berlin, Heidelberg, 2006.
- 868 Frka, S., Kozarac, Z., and Čosović, B.: Characterization and seasonal variations of surface active
869 substances in the natural sea surface micro-layers of the coastal Middle Adriatic stations,



- 870 Estuarine, coastal and shelf science, 85, 555-564,
871 <https://doi.org/10.1016/j.ecss.2009.09.023>, 2009.
- 872 Frossard, A. A., Gérard, V., Duplessis, P., Kinsey, J. D., Lu, X., Zhu, Y., Bisgrove, J., Maben, J. R.,
873 Long, M. S., Chang, R., Beaupré, S., Kieber, D. J., Keene, W. C., Nozière, B., and Cohen,
874 R. C.: Properties of seawater surfactants associated with primary marine aerosol particles
875 produced by bursting bubbles at a model air-sea interface, *Environmental Science &*
876 *Technology*, 53, 9407-9417, 10.1021/acs.est.9b02637, 2019.
- 877 Gašparović, B. and Čosović, B.: Surface-active properties of organic matter in the North Adriatic
878 Sea, *Estuarine, Coastal and Shelf Science*, 58, 555-566, [https://doi.org/10.1016/S0272-](https://doi.org/10.1016/S0272-7714(03)00133-1)
879 [7714\(03\)00133-1](https://doi.org/10.1016/S0272-7714(03)00133-1), 2003.
- 880 Gašparović, B., Plavšić, M., Čosović, B., and Saliot, A.: Organic matter characterization in the sea
881 surface microlayers in the subarctic Norwegian fjords region, *Marine Chemistry*, 105, 1-
882 14, <https://doi.org/10.1016/j.marchem.2006.12.010>, 2007.
- 883 Gérard, V., Nozière, B., Baduel, C., Fine, L., Frossard, A. A., and Cohen, R. C.: Anionic, cationic,
884 and nonionic surfactants in atmospheric aerosols from the Baltic Coast at Asko, Sweden:
885 Implications for cloud droplet activation, *Environmental Science & Technology*, 50, 2974-
886 2982, 10.1021/acs.est.5b05809, 2016.
- 887 Gómez-Consarnau, L., Raven, J. A., Levine, N. M., Cutter, L. S., Wang, D., Seegers, B., Aristegui,
888 J., Fuhrman, J. A., Gasol, J. M., and Sañudo-Wilhelmy, S. A.: Microbial rhodopsins are
889 major contributors to the solar energy captured in the sea, *Science Advances*, 5, eaaw8855,
890 doi:10.1126/sciadv.aaw8855, 2019.
- 891 González-Miguéns, R., Gálvez-Morante, À., Skamnelou, M., Antó, M., Casacuberta, E., Richter,
892 D. J., Lara, E., Vaultot, D., del Campo, J., and Ruiz-Trillo, I.: A novel taxonomic database
893 for eukaryotic mitochondrial cytochrome oxidase subunit I gene (eKOI), with a focus on
894 protists diversity, *Database*, 2025, 10.1093/database/baaf057, 2025.
- 895 Grote, J., Thrash, J. C., Huggett, M. J., Landry, Z. C., Carini, P., Giovannoni, S. J., and Rappé, M.
896 S.: Streamlining and Core Genome Conservation among Highly Divergent Members of the
897 SAR11 Clade, *mBio*, 3, 10.1128/mbio.00252-00212, doi:10.1128/mbio.00252-12, 2012.
- 898 Guillou, L., Bachar, D., Audic, S., Bass, D., Berney, C., Bittner, L., Boutte, C., Burgaud, G., de
899 Vargas, C., Decelle, J., del Campo, J., Dolan, J. R., Dunthorn, M., Edvardsen, B.,
900 Holzmann, M., Kooistra, W. H. C. F., Lara, E., Le Bescot, N., Logares, R., Mahé, F.,
901 Massana, R., Montresor, M., Morard, R., Not, F., Pawlowski, J., Probert, I., Sauvadet, A.-
902 L., Siano, R., Stoeck, T., Vaultot, D., Zimmermann, P., and Christen, R.: The Protist
903 Ribosomal Reference database (PR2): a catalog of unicellular eukaryote Small Sub-Unit
904 rRNA sequences with curated taxonomy, *Nucleic Acids Research*, 41, D597-D604,
905 10.1093/nar/gks1160, 2012.
- 906 Hardy, J. T.: The sea surface microlayer: Biology, chemistry and anthropogenic enrichment,
907 *Progress in Oceanography*, 11, 307-328, [https://doi.org/10.1016/0079-6611\(82\)90001-5](https://doi.org/10.1016/0079-6611(82)90001-5),
908 1982.
- 909 Hoffman, E. J. and Duce, R. A.: Factors influencing the organic carbon content of marine aerosols:
910 A laboratory study, *Journal of Geophysical Research* (1896-1977), 81, 3667-3670,
911 <https://doi.org/10.1029/JC081i021p03667>, 1976.
- 912 Hudson, J. M., MacDonald, D. J., Estes, E. R., and Luther, G. W.: A durable and inexpensive pump
913 profiler to monitor stratified water columns with high vertical resolution, *Talanta*, 199, 415-
914 424, 10.1016/j.talanta.2019.02.076, 2019.



- 915 Hudson, N., Baker, A., Ward, D., Reynolds, D. M., Brunson, C., Carliell-Marquet, C., and
916 Browning, S.: Can fluorescence spectrometry be used as a surrogate for the Biochemical
917 Oxygen Demand (BOD) test in water quality assessment? An example from South West
918 England, *Science of the Total Environment*, 391, 149-158,
919 10.1016/j.scitotenv.2007.10.054, 2008.
- 920 Huguet, A., Vacher, L., Relexans, S., Saubusse, S., Froidefond, J. M., and Parlanti, E.: Properties
921 of fluorescent dissolved organic matter in the Gironde Estuary, *Organic Geochemistry*, 40,
922 706-719, <https://doi.org/10.1016/j.orggeochem.2009.03.002>, 2009.
- 923 IOCCG: Phytoplankton Functional Types from Space, Reports of the International Ocean-Colour
924 Coordinating Group, IOCCG, Dartmouth, Canada 2014.
- 925 Ishii, A., Shan, J., Sheng, X., Kim, E., Watanabe, A., Yokono, M., Noda, C., Song, C., Murata, K.,
926 Liu, Z., and Minagawa, J.: The photosystem I supercomplex from a primordial green alga
927 *Ostreococcus tauri* harbors three light-harvesting complex trimers, *eLife*, 12, e84488,
928 10.7554/eLife.84488, 2023.
- 929 Jardak, K., Drogui, P., and Daghrir, R.: Surfactants in aquatic and terrestrial environment:
930 occurrence, behavior, and treatment processes, *Environmental Science and Pollution*
931 *Research*, 23, 3195-3216, 10.1007/s11356-015-5803-x, 2016.
- 932 Jeong, H. J., Yoo, Y. D., Seong, K. A., Kim, J. H., Park, J. Y., Kim, S., Lee, S. H., Ha, J. H., and
933 Yih, W. H.: Feeding by the mixotrophic red-tide dinoflagellate *Gonyaulax polygramma*:
934 mechanisms, prey species, effects of prey concentration, and grazing impact, *Aquatic*
935 *Microbial Ecology*, 38, 249-257, 2005.
- 936 Kozich, J. J., Westcott, S. L., Baxter, N. T., Highlander, S. K., and Schloss, P. D.: Development of
937 a Dual-Index Sequencing Strategy and Curation Pipeline for Analyzing Amplicon
938 Sequence Data on the MiSeq Illumina Sequencing Platform, *Appl Environ Microb*, 79,
939 5112-5120, 10.1128/Aem.01043-13, 2013.
- 940 Kujawinski, E. B., Farrington, J. W., and Moffett, J. W.: Evidence for grazing-mediated production
941 of dissolved surface-active material by marine protists, *Marine Chemistry*, 77, 133-142,
942 [https://doi.org/10.1016/S0304-4203\(01\)00082-2](https://doi.org/10.1016/S0304-4203(01)00082-2), 2002.
- 943 Kurata, N., Vella, K., Hamilton, B., Shivji, M., Soloviev, A., Matt, S., Tartar, A., and Perrie, W.:
944 Surfactant-associated bacteria in the near-surface layer of the ocean, *Scientific Reports*, 6,
945 10.1038/srep19123, 2016.
- 946 Lang-Yona, N., Flores, J. M., Haviv, R., Alberti, A., Poulain, J., Belser, C., Trainic, M., Gat, D.,
947 Ruscheweyh, H.-J., Wincker, P., Sunagawa, S., Rudich, Y., Koren, I., and Vardi, A.:
948 Terrestrial and marine influence on atmospheric bacterial diversity over the north Atlantic
949 and Pacific Oceans, *Communications Earth & Environment*, 3, 121, 10.1038/s43247-022-
950 00441-6, 2022.
- 951 Lawaetz, A. J. and Stedmon, C. A.: Fluorescence Intensity Calibration Using the Raman Scatter
952 Peak of Water, *Appl. Spectrosc.*, 63, 936-940, 2009.
- 953 Lechtenfeld, O. J., Koch, B. P., Gašparović, B., Frka, S., Witt, M., and Kattner, G.: The influence
954 of salinity on the molecular and optical properties of surface microlayers in a karstic
955 estuary, *Marine Chemistry*, 150, 25-38, <https://doi.org/10.1016/j.marchem.2013.01.006>,
956 2013.
- 957 Li, A., Stoecker, D. K., and Coats, D. W.: Mixotrophy in gyrodinium galatheanum
958 (DINOPHYCEAE): grazing responses to light intensity and inorganic nutrients*, *Journal*
959 *of Phycology*, 36, 33-45, <https://doi.org/10.1046/j.1529-8817.2000.98076.x>, 2000.



- 960 Li, Y.-Y., Chen, X.-H., Xie, Z.-X., Li, D.-X., Wu, P.-F., Kong, L.-F., Lin, L., Kao, S.-J., and Wang,
961 D.-Z.: Bacterial Diversity and Nitrogen Utilization Strategies in the Upper Layer of the
962 Northwestern Pacific Ocean, *Front Microbiol*, Volume 9 - 2018,
963 10.3389/fmicb.2018.00797, 2018.
- 964 Lichtenberg, M., Cartaxana, P., and Köhl, M.: Vertical Migration Optimizes Photosynthetic
965 Efficiency of Motile Cyanobacteria in a Coastal Microbial Mat, *Frontiers in Marine
966 Science*, Volume 7 - 2020, 10.3389/fmars.2020.00359, 2020.
- 967 Liu, X., Zhang, Y., Sun, H., Tan, S., and Zhang, X.-H.: Highly active bacterial DMSP metabolism
968 in the surface microlayer of the eastern China marginal seas, *Front Microbiol*, Volume 14
969 - 2023, 10.3389/fmicb.2023.1135083, 2023.
- 970 López-Pérez, M., Gonzaga, A., Martín-Cuadrado, A.-B., Onyshchenko, O., Ghavidel, A., Ghai, R.,
971 and Rodríguez-Valera, F.: Genomes of surface isolates of *Alteromonas macleodii*: the life
972 of a widespread marine opportunistic copiotroph, *Scientific Reports*, 2, 696,
973 10.1038/srep00696, 2012.
- 974 Maie, N., Scully, N. M., Pisani, O., and Jaffé, R.: Composition of a protein-like fluorophore of
975 dissolved organic matter in coastal wetland and estuarine ecosystems, *Water Research*, 41,
976 563-570, 10.1016/j.watres.2006.11.006, 2007.
- 977 Maneerat, S., Bamba, T., Harada, K., Kobayashi, A., Yamada, H., and Kawai, F.: A novel crude oil
978 emulsifier excreted in the culture supernatant of a marine bacterium, *Myroides* sp. strain
979 SM1, *Applied Microbiology and Biotechnology*, 70, 254-259, 10.1007/s00253-005-0050-
980 6, 2006.
- 981 Martin, S. F., Doherty, M. K., Salvo-Chirnside, E., Tammireddy, S. R., Liu, J., Le Bihan, T., and
982 Whitfield, P. D.: Surviving Starvation: Proteomic and Lipidomic Profiling of Nutrient
983 Deprivation in the Smallest Known Free-Living Eukaryote, *Metabolites*, 10, 273, 2020.
- 984 McKnight, D. M., Boyer, E. W., Westerhoff, P. K., Doran, P. T., Kulbe, T., and Andersen, D. T.:
985 Spectrofluorometric characterization of dissolved organic matter for indication of
986 precursor organic material and aromaticity, *Limnology and Oceanography*, 46, 38-48,
987 <https://doi.org/10.4319/lo.2001.46.1.0038>, 2001.
- 988 Morales-Guzmán, D., Martínez-Morales, F., Bertrand, B., Rosas-Galván, N. S., Curiel-Maciél, N.
989 F., Teymennet-Ramírez, K. V., Mazón-Román, L. E., Licea-Navarro, A. F., and Trejo-
990 Hernández, M. R.: Microbial prospection of communities that produce biosurfactants from
991 the water column and sediments of the Gulf of Mexico, *Biotechnology and Applied
992 Biochemistry*, 68, 1202-1215, <https://doi.org/10.1002/bab.2042>, 2021.
- 993 Mouw, C. B., Hardman-Mountford, N. J., Alvain, S., Bracher, A., Brewin, R. J. W., Bricaud, A.,
994 Ciotti, A. M., Devred, E., Fujiwara, A., Hirata, T., Hirawake, T., Kostadinov, T. S., Roy, S.,
995 and Uitz, J.: A Consumer's Guide to Satellite Remote Sensing of Multiple Phytoplankton
996 Groups in the Global Ocean, *Frontiers in Marine Science*, Volume 4 - 2017,
997 10.3389/fmars.2017.00041, 2017.
- 998 Murphy, K. R., Stedmon, C. A., Wenig, P., and Bro, R.: OpenFluor– an online spectral library of
999 auto-fluorescence by organic compounds in the environment, *Analytical Methods*, 6, 658-
1000 661, 10.1039/C3AY41935E, 2014.
- 1001 Oggerin, M., Viver, T., Brüwer, J., Voß, D., García-Llorca, M., Zielinski, O., Orellana, L. H., and
1002 Fuchs, B. M.: Niche differentiation within bacterial key-taxa in stratified surface waters of
1003 the Southern Pacific Gyre, *The ISME Journal*, 18, 10.1093/ismej/wrae155, 2024.



- 1004 Ohno, T.: Fluorescence Inner-Filtering Correction for Determining the Humification Index of
1005 Dissolved Organic Matter, *Environmental Science & Technology*, 36, 742-746,
1006 10.1021/es0155276, 2002.
- 1007 Oksanen, J., Blanchet, F. G., Kindt, R., Legendre, P., Minchin, P. R., O'Hara, R. B., Simpson, G.
1008 L., Solymos, P., Stevens, M. H. H., and Wagner, H.: *vegan: Community Ecology Package*,
1009 University of Helsinki [code], 2022.
- 1010 Ouyang, T. Y., Mckenna, A. M., and Wozniak, A. S.: Storm-driven hydrological, seasonal, and land
1011 use/land cover impact on dissolved organic matter dynamics in a mid-Atlantic, USA coastal
1012 plain river system characterized by 21 T FT-ICR mass spectrometry, *Front Env Sci-Switz*,
1013 12, 10.3389/fenvs.2024.1379238, 2024.
- 1014 Palovaara, J., Akram, N., Baltar, F., Bunse, C., Forsberg, J., Pedrós-Alió, C., González, J. M., and
1015 Pinhassi, J.: Stimulation of growth by proteorhodopsin phototrophy involves regulation of
1016 central metabolic pathways in marine planktonic bacteria, *Proceedings of the National
1017 Academy of Sciences*, 111, E3650-E3658, doi:10.1073/pnas.1402617111, 2014.
- 1018 Pedersen, T. L.: *ggraph: An Implementation of Grammar of Graphics for Graphs and Networks*,
1019 *Data-imaginist* [code], 2022.
- 1020 Pereira, R., Ashton, I., Sabbaghzadeh, B., Shutler, J. D., and Upstill-Goddard, R. C.: Reduced air-
1021 sea CO₂ exchange in the Atlantic Ocean due to biological surfactants, *Nature Geoscience*,
1022 11, 492+, 10.1038/s41561-018-0136-2, 2018.
- 1023 Poehlein, A., Kusian, B., Friedrich, B., Daniel, R., and Bowien, B.: Complete Genome Sequence
1024 of the Type Strain *Cupriavidus necator* N-1, *Journal of Bacteriology*, 193, 5017-5017,
1025 doi:10.1128/jb.05660-11, 2011.
- 1026 Pucher, M., Wunsch, U., Weigelhofer, G., Murphy, K., Hein, T., and Graeber, D.: *staRdom*:
1027 Versatile Software for Analyzing Spectroscopic Data of Dissolved Organic Matter in R,
1028 *Water*, 11, 2366, 2019.
- 1029 Quast, C., Pruesse, E., Yilmaz, P., Gerken, J., Schweer, T., Yarza, P., Peplies, J., and Glöckner, F.
1030 O.: The SILVA ribosomal RNA gene database project: improved data processing and web-
1031 based tools, *Nucleic Acids Research*, 41, D590-D596, 10.1093/nar/gks1219, 2012.
- 1032 Rahlff, J., Stolle, C., Giebel, H.-A., Mustaffa, N. I. H., Wurl, O., and P. R. Herlemann, D.: Sea
1033 foams are ephemeral hotspots for distinctive bacterial communities contrasting sea-surface
1034 microlayer and underlying surface water, *FEMS Microbiology Ecology*, 97,
1035 10.1093/femsec/fiab035, 2021.
- 1036 Rai, S., Acharya-Siwakoti, E., Kafle, A., Devkota, H. P., and Bhattarai, A.: Plant-Derived
1037 Saponins: A Review of Their Surfactant Properties and Applications, *Sci*, 3, 44, 2021.
- 1038 Ramfelt, O., Freel, K. C., Tucker, S. J., Nigro, O. D., and Rappé, M. S.: Isolate-anchored
1039 comparisons reveal evolutionary and functional differentiation across SAR86 marine
1040 bacteria, *The ISME Journal*, 18, 10.1093/ismejo/wrae227, 2024.
- 1041 Ruff, S. E., de Angelis, I. H., Mullis, M., Payet, J. P., Magnabosco, C., Lloyd, K. G., Sheik, C. S.,
1042 Steen, A. D., Shipunova, A., Morozov, A., Reese, B. K., Bradley, J. A., Lemonnier, C.,
1043 Schrenk, M. O., Joye, S. B., Huber, J. A., Probst, A. J., Morrison, H. G., Sogin, M. L.,
1044 Ladau, J., and Colwell, F.: A global comparison of surface and subsurface microbiomes
1045 reveals large-scale biodiversity gradients, and a marine-terrestrial divide, *Science
1046 Advances*, 10, eadq0645, doi:10.1126/sciadv.adq0645, 2024.
- 1047 Salonen, K., Järvinen, M., Aalto, T., Likolammi, M., Lindblom, V., Münster, U., and Sarvala, J.:
1048 Dynamic adaptation of phytoplankton vertical migration to changing grazing and nutrient
1049 conditions, *Hydrobiologia*, 851, 3639-3663, 10.1007/s10750-024-05526-1, 2024.



- 1050 Sharp, J. H., Benner, R., Bennett, L., Carlson, C. A., Dow, R., and Fitzwater, S. E.: Re-evaluation
1051 of high temperature combustion and chemical oxidation measurements of dissolved
1052 organic carbon in seawater, *Limnology and Oceanography*, 38, 1774-1782,
1053 <https://doi.org/10.4319/lo.1993.38.8.1774>, 1993.
- 1054 Siano, R., Alves-de-Souza, C., Foulon, E., Bendif, E. M., Simon, N., Guillou, L., and Not, F.:
1055 Distribution and host diversity of Amoebozoa parasites across oligotrophic waters of
1056 the Mediterranean Sea, *Biogeosciences*, 8, 267-278, 10.5194/bg-8-267-2011, 2011.
- 1057 Sousoni, D.: Marine phototroph-heterotroph interactions, University of Warwick, 2018.
- 1058 Stedmon, C. A. and Bro, R.: Characterizing dissolved organic matter fluorescence with parallel
1059 factor analysis: a tutorial, *Limnology and Oceanography: Methods*, 6, 572-579,
1060 <https://doi.org/10.4319/lom.2008.6.572>, 2008.
- 1061 Stedmon, C. A. and Markager, S.: Tracing the production and degradation of autochthonous
1062 fractions of dissolved organic matter by fluorescence analysis, *Limnology and
1063 Oceanography*, 50, 1415-1426, <https://doi.org/10.4319/lo.2005.50.5.1415>, 2005.
- 1064 STOECK, T., BASS, D., NEBEL, M., CHRISTEN, R., JONES, M. D. M., BREINER, H.-W., and
1065 RICHARDS, T. A.: Multiple marker parallel tag environmental DNA sequencing reveals a
1066 highly complex eukaryotic community in marine anoxic water, *Molecular Ecology*, 19, 21-
1067 31, <https://doi.org/10.1111/j.1365-294X.2009.04480.x>, 2010.
- 1068 Stoecker, D. K., Hansen, P. J., Caron, D. A., and Mitra, A.: Mixotrophy in the Marine Plankton,
1069 *Annual Review of Marine Science*, 9, 311-335, [https://doi.org/10.1146/annurev-marine-
1070 010816-060617](https://doi.org/10.1146/annurev-marine-010816-060617), 2017.
- 1071 Swan, B. K., Tupper, B., Sczyrba, A., Lauro, F. M., Martinez-Garcia, M., González, J. M., Luo,
1072 H., Wright, J. J., Landry, Z. C., Hanson, N. W., Thompson, B. P., Poulton, N. J.,
1073 Schwientek, P., Acinas, S. G., Giovannoni, S. J., Moran, M. A., Hallam, S. J., Cavicchioli,
1074 R., Woyke, T., and Stepanauskas, R.: Prevalent genome streamlining and latitudinal
1075 divergence of planktonic bacteria in the surface ocean, *Proceedings of the National
1076 Academy of Sciences*, 110, 11463-11468, doi:10.1073/pnas.1304246110, 2013.
- 1077 Tastassa, A. C., Dubowski, Y., Argaman Meirovich, O., Kuzmenkov, I., and Lang-Yona, N.:
1078 Selective Ocean–Atmosphere Bacterial Flux Through the Pacific Sea Surface Microlayer,
1079 *ACS ES&T Air*, 2, 837-846, 10.1021/acsestair.4c00302, 2025.
- 1080 Taylor, J. D. and Cunliffe, M.: High-throughput sequencing reveals neustonic and planktonic
1081 microbial eukaryote diversity in coastal waters, *Journal of Phycology*, 50, 960-965,
1082 <https://doi.org/10.1111/jpy.12228>, 2014.
- 1083 van den Boogaart, K. G. and Tolosana-Delgado, R.: “compositions”: A unified R package to
1084 analyze compositional data, *Computers & Geosciences*, 34, 320-338,
1085 <https://doi.org/10.1016/j.cageo.2006.11.017>, 2008.
- 1086 Van Mooy, B. A. S., Rocap, G., Fredricks, H. F., Evans, C. T., and Devol, A. H.: Sulfolipids
1087 dramatically decrease phosphorus demand by picocyanobacteria in oligotrophic marine
1088 environments, *Proceedings of the National Academy of Sciences*, 103, 8607-8612,
1089 doi:10.1073/pnas.0600540103, 2006.
- 1090 Wilhelm, R. C.: Following the terrestrial tracks of Caulobacter - redefining the ecology of a reputed
1091 aquatic oligotroph, *The ISME Journal*, 12, 3025-3037, 10.1038/s41396-018-0257-z, 2018.
- 1092 Williams, C. J., Yamashita, Y., Wilson, H. F., Jaffé, R., and Xenopoulos, M. A.: Unraveling the
1093 role of land use and microbial activity in shaping dissolved organic matter characteristics
1094 in stream ecosystems, *Limnology and Oceanography*, 55, 1159-1171,
1095 [10.4319/lo.2010.55.3.1159](https://doi.org/10.4319/lo.2010.55.3.1159), 2010.



- 1096 Wilson, T. W., Ladino, L. A., Alpert, P. A., Breckels, M. N., Brooks, I. M., Browse, J., Burrows, S.
1097 M., Carslaw, K. S., Huffman, J. A., Judd, C., Kilhau, W. P., Mason, R. H., McFiggans, G.,
1098 Miller, L. A., Nájera, J. J., Polishchuk, E., Rae, S., Schiller, C. L., Si, M., Temprado, J. V.,
1099 Whale, T. F., Wong, J. P. S., Wurl, O., Yakobi-Hancock, J. D., Abbatt, J. P. D., Aller, J. Y.,
1100 Bertram, A. K., Knopf, D. A., and Murray, B. J.: A marine biogenic source of atmospheric
1101 ice-nucleating particles, *Nature*, 525, 234-238, 10.1038/nature14986, 2015.
- 1102 Wurl, O., Wurl, E., Miller, L., Johnson, K., and Vagle, S.: Formation and global distribution of sea-
1103 surface microlayers, *Biogeosciences*, 8, 121-134, 10.5194/bg-8-121-2011, 2011.
- 1104 Wurl, O., Bird, K., Cunliffe, M., Landing, W. M., Miller, U., Mustaffa, N. I. H., Ribas-Ribas, M.,
1105 Witte, C., and Zappa, C. J.: Warming and Inhibition of Salinization at the Ocean's Surface
1106 by Cyanobacteria, *Geophysical Research Letters*, 45, 4230-4237,
1107 <https://doi.org/10.1029/2018GL077946>, 2018.
- 1108 Yamashita, Y., Fichot, C. G., Shen, Y., Jaffé, R., and Benner, R.: Linkages among fluorescent
1109 dissolved organic matter, dissolved amino acids and lignin-derived phenols in a river-
1110 influenced ocean margin, *Frontiers in Marine Science*, Volume 2 - 2015,
1111 10.3389/fmars.2015.00092, 2015.
- 1112 Zäncker, B., Cunliffe, M., and Engel, A.: Bacterial Community Composition in the Sea Surface
1113 Microlayer Off the Peruvian Coast, *Front Microbiol*, Volume 9 - 2018,
1114 10.3389/fmicb.2018.02699, 2018.
- 1115 Zäncker, B., Cunliffe, M., and Engel, A.: Eukaryotic community composition in the sea surface
1116 microlayer across an east-west transect in the Mediterranean Sea, *Biogeosciences*, 18,
1117 2107-2118, 10.5194/bg-18-2107-2021, 2021.
- 1118 Zhang, Z. B., Cai, W. J., Liu, L. S., Liu, C. Y., and Chen, F. Z.: Direct determination of thickness
1119 of sea surface microlayer using a pH microelectrode at original location, *Sci China Ser B*,
1120 46, 339-351, 10.1360/02yb0192, 2003.
- 1121 Zutic, V., Cosovic, B., Marcenko, E., Bihari, N., and Krsinic, F.: Surfactant production by marine-
1122 phytoplankton, *Marine Chemistry*, 10, 505-520, 10.1016/0304-4203(81)90004-9, 1981.
- 1123